Horizon 2020

flora **robotica**

Societies of Symbiotic Robot-Plant Bio-Hybrids as Social Architectural Artifacts

Deliverable D1.3

Plant-robot interaction mechanisms and distributed actuation system

Date of preparation: 2018/03/31	**Revision: 1 (r843)**
Start date of project: 2015/04/01	**Duration: 48 months**
Project coordinator: UzL	**Classification: public**
Partners: *lead:* **ITU**	*contribution:* **CYB, CITA, UzL, UNIGRAZ, AMU**
Project website:	http://florarobotica.eu/

H2020-FETPROACT-2014

DELIVERABLE SUMMARY SHEET

Grant agreement number:	640959
Project acronym:	*flora robotica*
Title:	Societies of Symbiotic Robot-Plant Bio-Hybrids as Social Architectural Artifacts

Deliverable N^o:	Deliverable D1.3
Due date:	M36
Delivery date:	2018/03/31

Name:	**Plant-robot interaction mechanisms and distributed actuation system**
Description:	Interaction between the three agent groups: structure, biological organisms, and robots is crucial for the development of plant-robot hybrid organisms in *flora robotica*. A broad range of hardware studies and developments has been investigated for such hybrid interactions. Here we present and evaluate interaction mechanisms separated into sensing and actuation between agent groups in distributed actuation systems. Interaction is understood as bidirectional; sensing and actuation which can take place these two ways between three distinct parts of the hybrid namely, robots, plants, and structures. Therefore we divide the field into a number of distinct (inter)actions as follows: Plants - Robots; Robots - Plants; Robots - Structures. Additionally, we will report on the progress on the production of the braided structures themselves before the beginning of their lifetime in the hybrid.

Partners owning:	**ITU**
Partners contributed:	**CYB, CITA, UzL, UNIGRAZ, AMU**
Made available to:	public

Contents

1 Introduction: Interaction Mechanisms of Robotic Symbiont

Interaction and actuation of structures takes place on several levels in *flora robotica*. Bidirectional interactions can be separated between three interacting parts: robot, braid structure, and plant. Furthermore we can distinguish between the production of braids and actuation during the braid's lifetime, while performing a task in a given hybrid with plants and robots. Interaction can also be separated into sensing, as part emitting information, and affecting as part of receiving information. To affect plants a number of techniques has been tested including light, hormones and vibration, some of which, in turn, can be used to provoke emission of signals for sensing technology to capture and record.

1.1 Actuation for manufacture

Production of braided structures was performed manually by hand initially. An exploration process of finding properties of various materials and at various scales of braids. Soon we realized the project would need to develop a number of research tools that could augment our capacity to search the field of braided structures both with regards to more intricate patterns as well as across various materials. A number of different physical prototype approaches were started, some showing greater potential and scalability than others. Finally we chose an approach making use of reconfigurable modules able of various assemblies while maintaining central control. With this reconfigurable machine we can produce braids with various patterns depending both on the physical configuration of the machine as well as the virtual programming of its actuators. We demonstrate how this machine produces braided structures in different topologies from various materials. Output is suitable in size for plants and can be used in future demonstrators.

1.2 Actuation during lifespan

Having settled on the concept of continuously braided fibrous structure as basis in the robotic symbiont we explore actuation on a number of scalar, topological, and directional levels. In some prototype experiments we focus on actuating plants seen from the braided structures, in others we actuate the braided structures using various mechanical actuators. For actuation of the braided structures themselves various approaches to kinetic actuation are tested: Cable-winch, thermo-plastic, thermal bi-metal and servo motor. To actuate plants, however, we have found alternative stimulation techniques of growth direction. We have tested light, hormone, and kinetics, such as wind and vibration from mechanical actuators. The following tasks are included in this deliverable: T1.3, T1.4, T1.5, although T1.4 and T1.5 are not yet finalized.

Braids consist of multiple similar members in a reciprocally constrained structure [2, 1, 7]. This makes them suitable for distributed actuation as the connections between members are topologically identical. This similarity makes a distributed paradigm suitable, as one type of actuator can be multiplied. For the vision of a social garden we envision an open ecology consisting of robots, plants, and humans able to sense and affect each other across time and space. To develop this vision we not only must develop generic sensors, but also computational methods to translate and convey data across structures, robots, plants, and humans. In turn, actions are instigated by various sources of data capture, creating an open-loop system of interactions.

1.3 Content overview

We are working on several distinct aspects of interactions in order to create an eco-system of plant-robot symbionts. In chapter 3 *Actuation: Robots-Structures*, we deliver results from a number of different actuation strategies for braided structures. Each approach seems to have promising advantages for different parts of the symbiont and for symbionts in different environments. In chapter 4 *Actuation: Robots-Plants*, we deliver results from a number of actuation strategies for plants, and conclude on their individual advantages. In chapter 5 *Sensing: Plants-Robots*, we deliver results from the *Phytosensing* System in technical and software perspective, and also results from the system in use sensing plants being subjected to external stimuli. Future demonstrators will integrate selected distributed and centralized actuation and sensing approaches presented here.

Prototype	**Activity**	**Direction**	**Partners**
Manufacturing	Actuation of control modules	Robot-Structure	ITU
Servo actuation	Energy capture	Robot-Robot	ITU
Cable actuation	Kinetic manipulation	Robot-Robot	ITU, CITA
SMA actuation	Kinetic manipulation	Robot-Robot	ITU, UzL
Light stimuli	Guidance of Growth	Robot-Plant	UzL, CITA, UNIGRAZ
Hormones stimuli	Guidance of Growth	Robot-Plant	AMU
Phytosensor	Sensing electrophysical signals in plants	Plant-Robot	CYBERTRONICA
Reinforcement	Growth reinforcement of structure	Plant-Structure	CITA, AMU

Table 1: An overview of the prototypes in *flora robotica* dealing with actuation and sensing.

2 Producing Braided Structures

Production of the braided structures can be separated from the actuation of the structures. Firstly, we will reintroduce the approach to production of braided structures, secondly we will report on our techniques for actuating the braided structures.

2.1 Controller for braiding machine to produce braided structures with varying topologies

Braided structures are used as both static and dynamic structures of various topologies and at various scales in *flora robotica*. We have identified some areas of application utilizing various materials, however the material variety can be broadened. With a braiding machine we hope to develop braided structures in various materials and varying topologies, however, we must have efficient controllers for the braiding machine to speed up the process of testing and producing. We have already designed a modular braiding robot for experimentation with braided structures (see D1.2). Recently we have also developed software to generate control commands for the braiding robot. The software for the machine is intuitive and easy to use, but not yet fail-safe.

The section *design and hardware* provides an overview of the mechanics, electronics, and control of actuation. The section *High level control software* provides an overview and insights to the software we have designed for the machine.

2.1.1. General functionality of modules

The functionality of the braiding machine is to transport carriers of filament in interweaving patterns to produce continuous reciprocal 2D or 3D braid structures. For the machine to be both cost-effective and versatile reconfiguration was essential as it allows for a variety of braid patterns from a minimum of hardware modules. The control software is designed for low level control of the microprocessor in the machine as well as for the high level control of reconfiguration, testing and simulation of carrier transportation. At this point we are not able to derive the machine configuration, and carrier instructions from an overall morphology and pattern, reversely we can test various carriers paths and visualize the braided output in simulation.

2.1.2. Mechanics

To move carriers in various crossing transportation routes four different types of reconfigurable modules were designed see Fig. 1. The (1) drivers of the braiding machine are designed to build tracks for the transportation routes while (2) junctions are routing the (3) carriers on their way through the machine. (4) borders prevent the carriers from falling off the open edges of the drivers. Transportation routes can be designed by assembling octagonal driver modules into strands. The number of possible configurations grow exponentially with the number of modules available. Drivers are equipped with a rotating sprocket on top transferring torsion between drivers. Hence, they turn clockwise and counter clockwise respectively. This sprocket design is combined with eight slots as seats for carriers to reduce parts, cost and complexity. The driver baseplate is octagonal allowing it to connect with a straight edge to adjacent modules. On top of this baseplate two circular plates of different diameter are fixed. The cross-section of these plates make up one half of the concave rail while adjacent rim, junction and driver modules make up the other half. Junctions brace and fasten the driver modules, and the servo motor on its bottom actuates the top switching tooth to route carriers passing by. All servos in the junctions are controlled from a 16-Channel 12-bit PWM/Servo Driver through I2C interface to a micro controller using Atmega2560 processor.

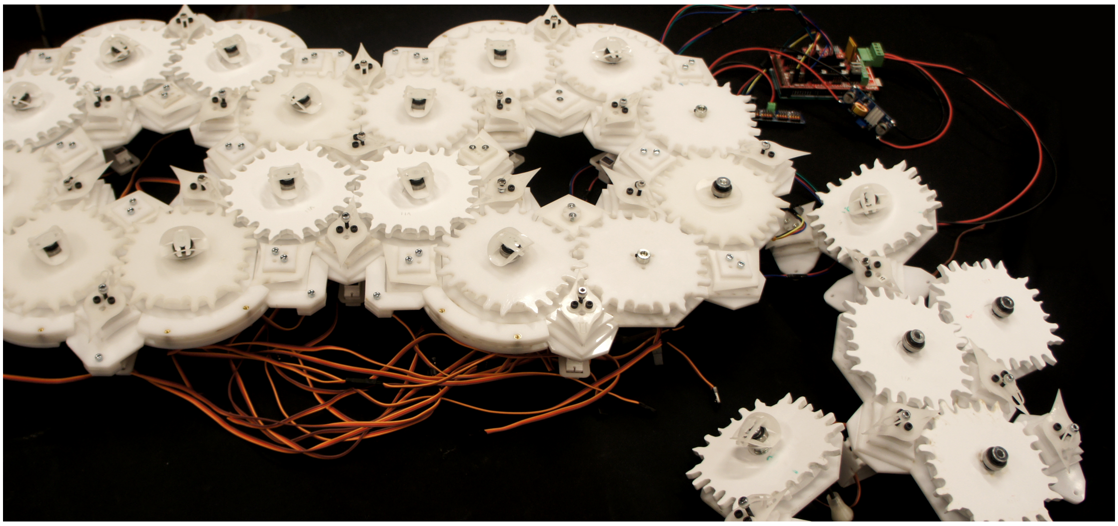

Figure 1: Reconfigurable hardware modules

2.1.3. Electronics

The Atmega2560 micro controller board acts as low level timer and is connected to a number of integrated circuits. (1) the aforementioned servo driver controlling all junctions. (2) an encoder with 6000 steps/revolution connected on one of the driver sprockets tracks position of the rotating sprockets constantly. We use a 12 bit encoder, the angle of rotation is represented by a number between 0 and 2048 (2^{11}). Therefore, the reading is accurate to about 0.09°. (3) a Rampsboard v.1.4 with up to 5 stepper motor drivers control up to 5 Nema 17 stepper motors which actuates the rotation of sprockets. Sprockets are directly mounted on the stepper motor axel to simplify design, ensure easy control of torque and manual overrule and to reduce damage at jamming by avoiding additional gears. A computer running the control software sends commands over serial port to the microcontroller. The commands buffer to the internal memory of the microcontroller, which in turn executes the servo commands in correlation with sprocket position.

Figure 2: Direction of messages passed between Software, Middleware and Hardware.

2.1.4. High level control software

This section provides an overview of control software functionality. User input configures the module layout, placement of carriers, and runs the machine. The resulting computation has a final output of the aforementioned strings that are sent over serial port to the micro controller of the braiding machine. The program has four main modes of operation. Mode 1 (Layout) This mode allows the user to (re)configure basic driver layout virtually. Mode 2 (tracks) allows the user to draw a number of tracks around this new configuration. Mode 3 (carriers) allows

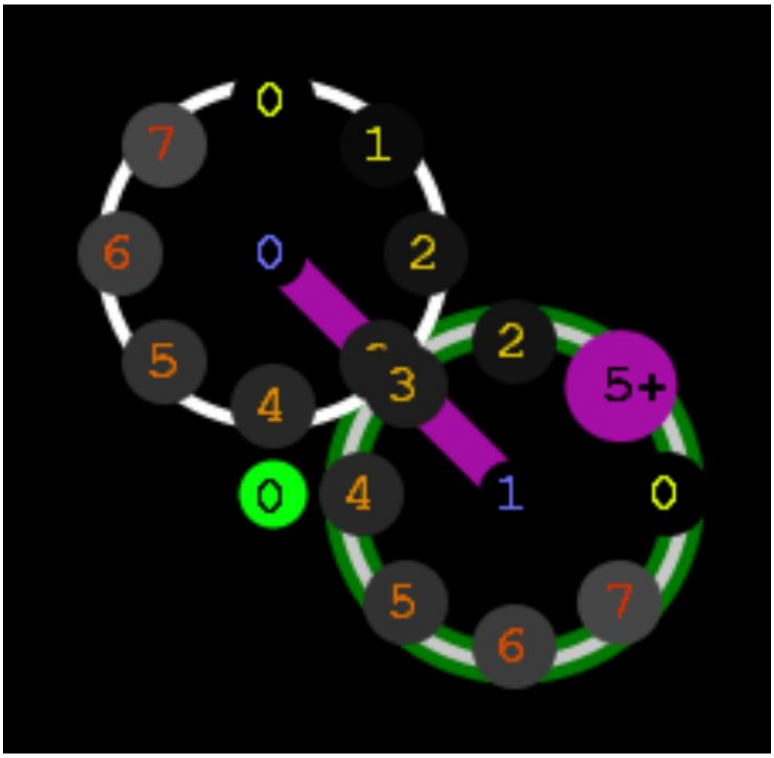

(a) This simple example shows two driver modules with a carrier moving on purple track numbered 5 in clockwise direction. As the carrier reach switch 0 it queries the switch whether it is connected to the next module on its track, namely driver 0. That is in this case true, therefore switch 0 is set to true, meaning the carrier turns right. As the carrier reaches the end of the track, it looks for the first driver in the track, to continue the circular movement.

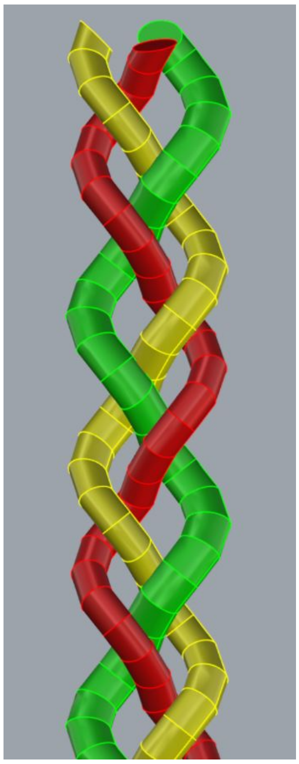

(b) Output from configuration shown to the left. The only difference is that three carriers have been moved around the two modules to create this basic Soutache braid.

Figure 3: Simplest possible configuration and the result in simulation

the user to insert carriers in positions on selected tracks in the new configuration. After having constructed the new physical configuration manually, Mode 4 (junctions) allows the user to build a map between junctions from the physical and the virtual machine.

Mode 1 (Layout): drivers are added or removed by the user. The program indicates the viable location closest to the cursor. As drivers are removed and added, the junctions are updated accordingly. To allow the user to experiment with various virtual layouts, eight different layouts can be loaded for modification. These layouts also contain information about tracks, which is also loaded upon opening a layout, see Fig. 2.

Mode 2 (Tracks): Tracks are created by the user. The tracks are defined for the carriers to be transported through the machine in a meaningful way. Tracks should always be drawn as a closed loop to ensure carriers can travel the track with their given direction repeatedly. In the program code, this means the carriers search for the next module in their given track, and at each junction decide for the junction to open or close before arriving. Carriers can travel either in positive or negative direction on the tracks.

Mode 3 (Carriers): Carriers are placed in drivers slots that belong to the currently selected track. Left and right mouse button determine which direction the carrier travels in the track. The insertion of carriers can be semi automated such that carriers are placed in starting locations that avoid collisions later on. Carriers placed in respective starting locations 0 through 7, never collide with carriers from other starting locations due to the logical numbering of slots. It can be observed that as a carrier placed in a location of a driver, moves into the same location number of the next driver. In other words, the difference of the remainder between the current position divided by eight, and position numbers remain the same throughout transportation, and they never find themselves in the same position.

Mode 4 (mapping): a map is built between the virtual numbering and the hardware numbering. The offset between the virtual number and the hardware address is recorded by sequentially flipping each physical junction, while asking the user to mark the corresponding virtual switch in software.

2.1.5. Operation

When a configuration is made and the carriers are placed virtually in tracks, the physical machine can be stepped through positions sequentially while it is being loaded with carriers. Once all physical carriers are in place of the virtual ones, the machine can continue the sequential steps. For each step, all drivers push carriers to the next position, at which point they run the computation shown in Fig. 5. At this computation they follow their assigned track, and loop to start when they meet end of the track. At any point the user can remove carriers from one track to follow another overlapping track. Such a shift of carriers from one track to another changes the braid pattern and thus the cross section of the produced braid. Changes in braid topologies can occur from this, such as bifurcations, splicing etc. The challenge of these operations is to avoid collisions between carriers. We have not yet designed an efficient algorithm for complete path planning and collision avoidance, however, a general strategy to avoid collisions is the initial placement of carriers in pairs of different starting locations. Fig. 4 shows how such a placement of carriers can be done automatically. The carriers are placed at every second module in every second location with alternating directions. Locations 0, 2, 4, and 6 are occupied but the remaining tracks can still use remaining locations 1, 3, 5, and 7 to run carriers without colliding with the purple carriers. To create a bifurcation of the large tubular braid, half of the carriers can be assigned a circular track in the left side, while the other half of the carriers are assigned to a circular track in the right side. If it is desired to fuse the two braids again, one shifts back on the purple track.

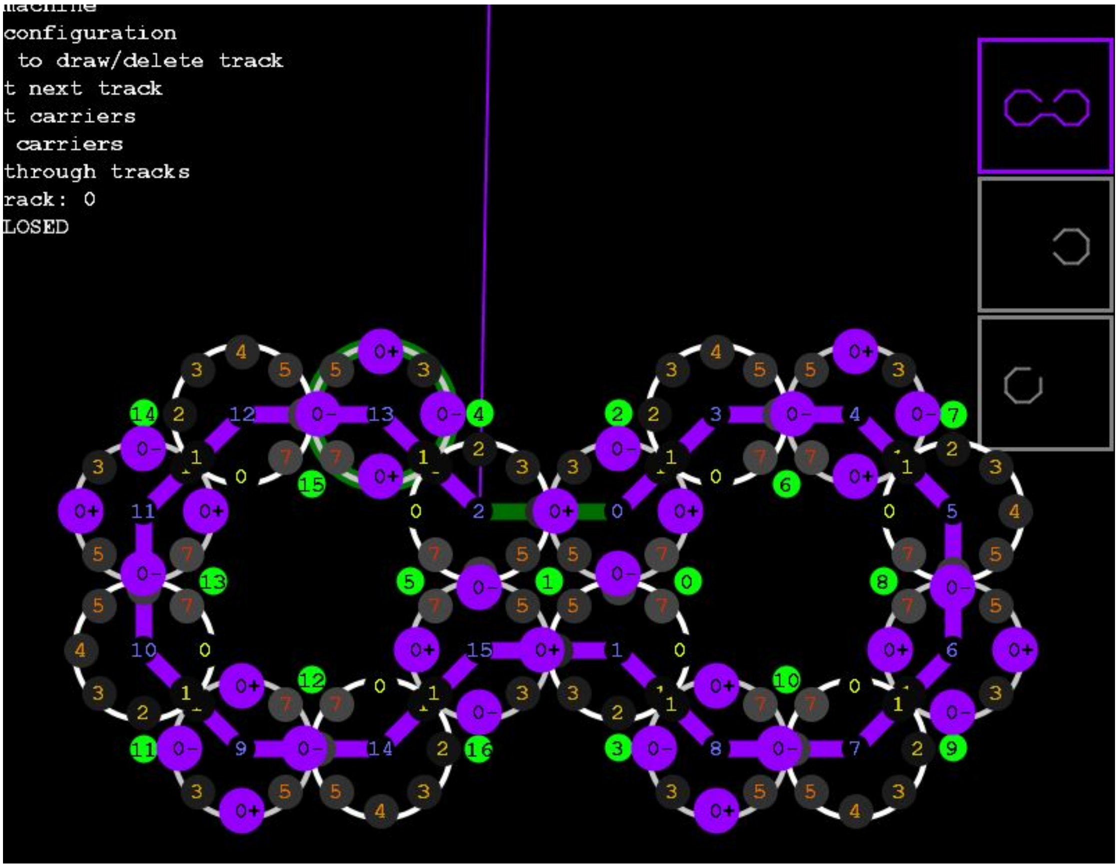

Figure 4: The software configuration for braiding either one large tubular braid (x32) or two smaller ones (x16). Purple lines indicate the track and purple dots mark respectively 0- and 0+ carriers placed on the purple track. Two other tracks are created for this configuration as seen at the top right side. The two tracks in gray, braid individual tubes of 16 members, while the purple track results in one large tube of 32 members.

2.2 Conclusions

We have reported on the increase of progress in the braiding machine, which is predominantly on the software and operation aspects. The machine is now highly functional and we have much to explore in terms of materials and patterns. We still have to generate more robust computational strategies to change from pattern to pattern during braiding in order to braid alternating topologies of braids, such as bifurcations, split tubes etc. The machine is soon ready for on-line publishing as open-source hardware. This will, in turn, make braiding available to engage a wide audience of researchers.

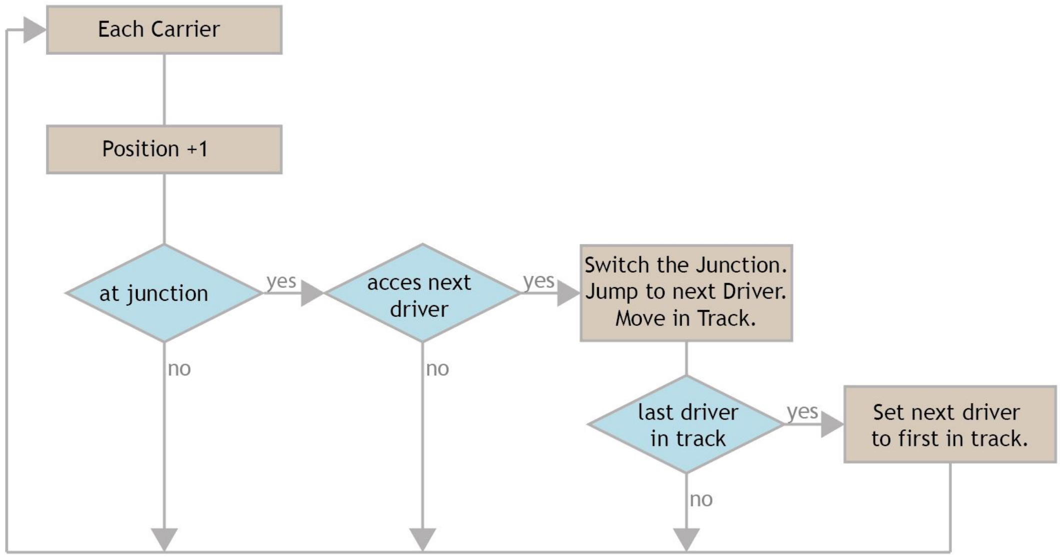

Figure 5: State diagram of a carrier moving one step in the machine, finding its way along a designated track.

3 Actuation: Robots - Structures

For the actuation of structures, we have experimented with different techniques. Each technique has different advantages and disadvantages. We discuss these in the sections following their description.

3.1 Stepper motor actuated triaxial strings for GFRP 3 DOF manipulator

Studies for the use of braid in dynamic structures began with an exploration of simple topologies and morphologies actuated manually to explore dynamic characteristics and gain insights into possible methods of actuation. Our initial prototype is shown in Fig. 6. It comprises 1 mm diameter GFRP filaments (Glass Fiber Reinforced Polymer) with a braid angle between 1 and 180 degrees. The base diameter of the braid is 200 mm. Filaments are connected to a plywood base for stability. The relaxed height of the braid is 750 mm. To explore the dynamic actuation potentials of the braid, we incorporated a tri-axial group of 3 vertical nylon wires interlaced through the GFRP rods and attached to the uppermost filament intersections. Interlacing helps keep these wires guided during actuation. The three wires are arranged with a 120 degree separation in plan to gain control within a hemi-spherical workspace. Tightening of an actuation wire introduces a point load pulling force resulting in directional bending distributed across the length of the braid. Co-ordinated actuation of two wires produces a turning movement. With all three wires actuated simultaneously, the body exhibits a contractile deformation that becomes more pronounced as the pulling force is increased. The stiffness of the GFRP rods allows the braid to naturally spring back into its relaxed state once actuation forces are removed. However, the use of tensile actuation wires prevents the exploitation of the extension dynamics that the braid is capable of producing. In this particular case, the extension will be limited due to the although to a limited degree due to the narrow diameter of the relaxed state. Through this

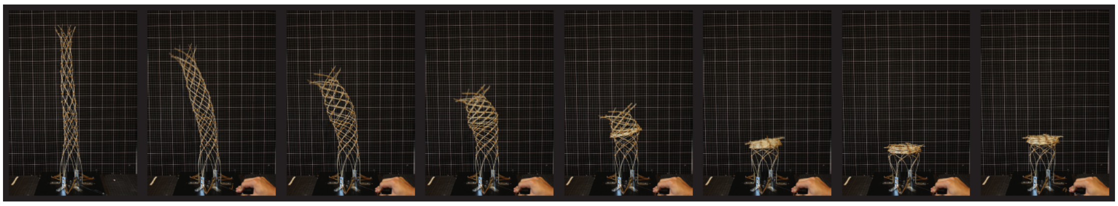

Figure 6: Elongation extremes possible in a braided fiberglass rod 3 DOF manipulator.

initial study we have determined that the braid exhibits morphological computation with the properties of a continuum body, and presents compelling opportunities for applying controlled actuation.

We have examined if the actuation and motion principles demonstrated in this prototype can be transferred to a larger scale construct. A second manually actuated prototype has been produced with a base diameter of 200 mm, relaxed height of 1200 mm, comprising 12 1 mm diameter GFRP filaments with a braid angle of 45 degrees resulting in a unit cell size of 110 mm measured across diagonals. Fig. 7 shows this prototype during construction (left) and completed (right). In this case, the braid has only been able to achieve self-structuring with the addition of elastic restraints located at filament intersections. The elastic restraints compress filaments together to enable self-bracing, but have sufficient compliance to allow for the local rotation and shear forces necessary to develop deformation behaviors within the braid body. In principle, the use of elastic restraints could be alleviated at this scale by increasing the density of interactions through the addition of more GFRP rods. However, this would impact the stiffness of the braid and require higher actuation forces to induce deformations. This prototype has been built to examine fabrication at larger scales, and has therefore not had wires added for actuation. However, it can be reported that through manual manipulation, the prototype exhibits high degrees of flexibility within a half-spherical workspace, with a range of movements including bending, contracting and extending.

To demonstrate controlled actuation of braided structures we have constructed a simple 3 degrees-of-freedom (DOF) manipulator using the same construction principles described above; 12 filaments of 1 mm diameter fiberglass rods with the intersections reinforced using elastic restraints (see Fig. 8). This structure is 0.7 m in height in a relaxed state, with a diameter between 0.15 m (top) and 0.22 m (bottom) only weighing 35 g. However, the supporting base weighs 1.9 kg.

In this demonstration we have transfered the external actuation approach used in the previous experiments; three nylon wires separated by 120 degrees that run up the length of the braid and attached to the upper-most filament intersections. In this case, the actuation wires are attached to winches located at the base, and actuation is induced by stepper motors. The motors are controlled from a Arduino Mega with a Ramps 1.4 Shield. A two dimensional cut of the work space is visualized in Fig. 9 and extends 360°around the base due to the 3 DOF. The payload capacity of the arm depends on how much deformation is acceptable, but allowing for only a few millimeters deflection from the unloaded position when the robot arm is at an extreme the arm can support 25 g. This manipulator demonstrates that we can built extremely light-weight, simple robot bodies. An absolute orientation sensor with three axis accelerometer, gyroscopic sensor and compass sensor was mounted to the end effector at the top of the structure.

After fusing the 9 data streams from the sensor, 3-DOF orientation of the crown could be traced and recorded. Given the alternative mechanical system of both structure and actuators, we did not attempt to make a controller with closed loop between sensor and stepper motors, instead we made an attempt to control the braid manipulator using an evolutionary robotics

Figure 7: A room-sized fiberglass rod braided manipulator; (left) in process of fabrication, (right) completed.

approach (see Fig. 10), in particular neuro-evolution of augmenting topologies (NEAT) [8]. Our rationale for investigating evolution of controllers is based on two arguments: 1) mechanical performance of overall morphology is sensitively dependent on changes in material characteristics, both temporary (e.g., live mechanical and environmental loads) and permanent (e.g., damage, material creep, long-term fatigue especially with the elastic restraints), 2) the premise of *flora robotica* anticipates operation in unstructured environments with symbiotic plant interaction; plants growing on an active scaffold such as the one described, could benefit from structural support in early stages of growth, but would progressively alter mechanical properties of the braid causing a predetermined controller to fail. NEAT is a valuable goal oriented optimization strategy commonly used to evolve robot behavior. Though the 3 degrees of freedom braided manipulator has a straightforward state space landscape, it has mainly been implemented with the idea of potentially expanding it to more complex braided structures. We did not manage to evolve a general controller for the braided structure and work on NEAT was discontinued in favor of simpler implementations of evolutionary algorithms.

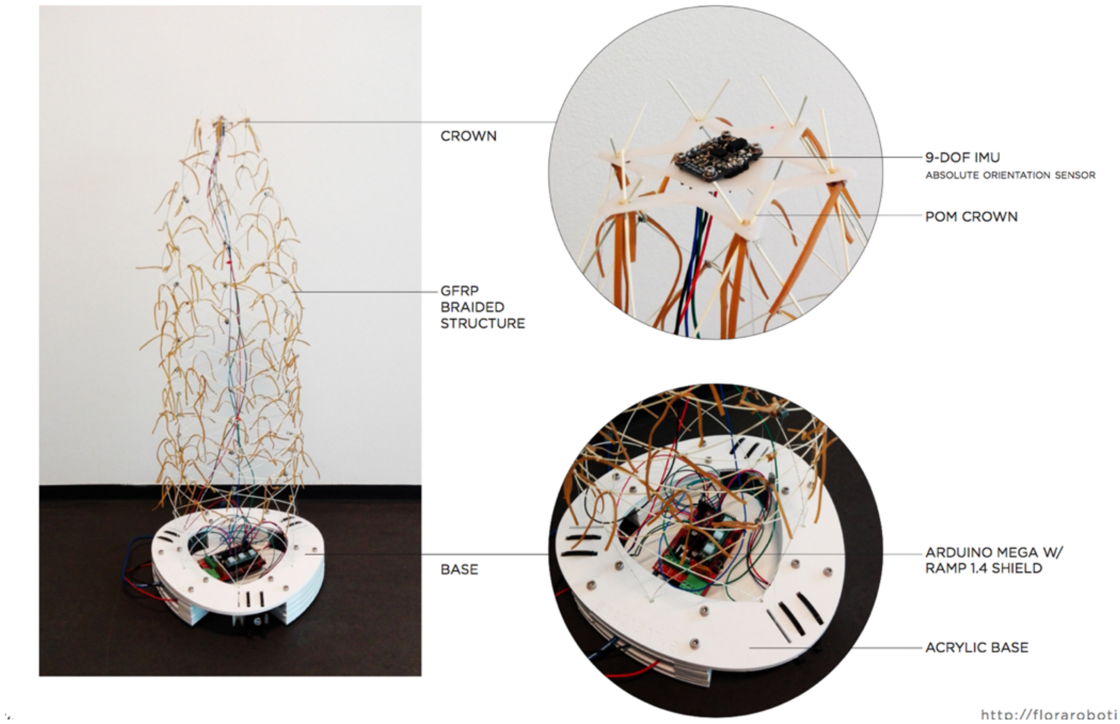

Figure 8: Hardware of the fiberglass rod 3 DOF manipulator.

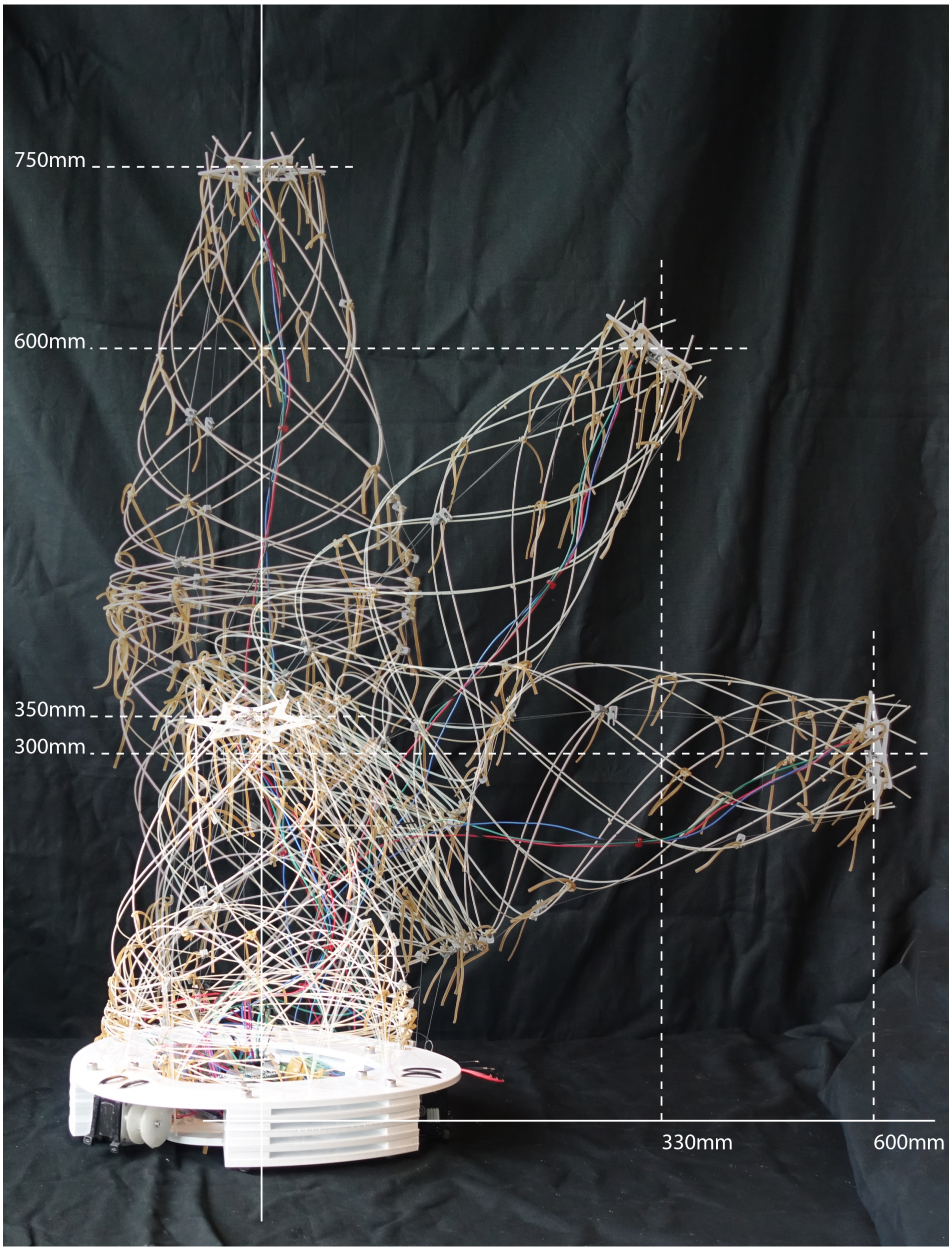

Figure 9: Hand-braided manipulator in 4 extreme positions. Workspace is half spherical and the manipulator reaches the points within this work-space with 3 DOF.

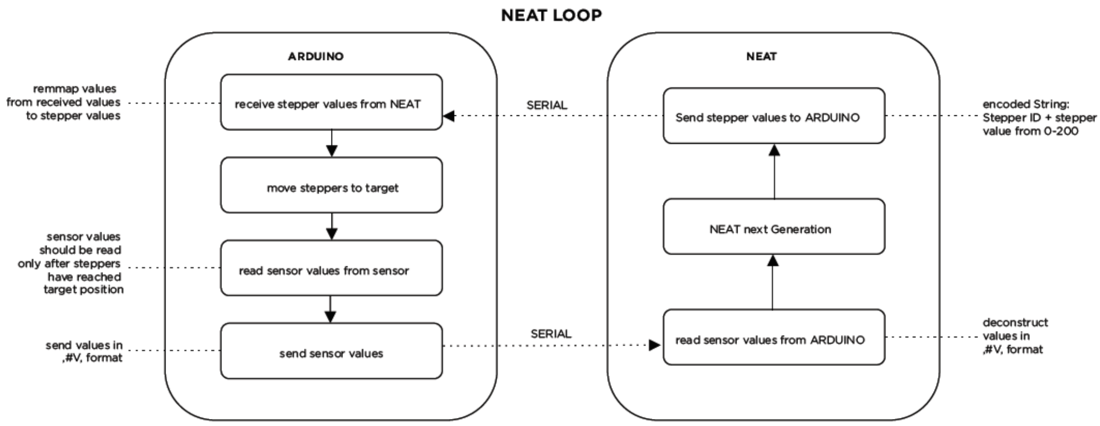

Figure 10: Support software for evolving behaviors of the manipulator

3.2 Servo actuated triaxial strings

To actuate tubular braided polypropylene (PP) strap structures we implemented triaxial strings actuated by servo motors. Tubular braided filament structures have a natural tendency to stretch in their length direction while reducing the cross section dimension because each individual member act as a spring relaxed in straight shape. Therefore we found it rational to work with fibrous transmission of forces in tension counteracting this extending spring behavior. To test this type of tensile transmission in combination with servo motors we implemented strings throughout the body of the before mentioned four limbed braid structure seen in Fig. 11. Such strings for actuation allow for flexible and compliant yet robust and static transmission between actuator and structure.

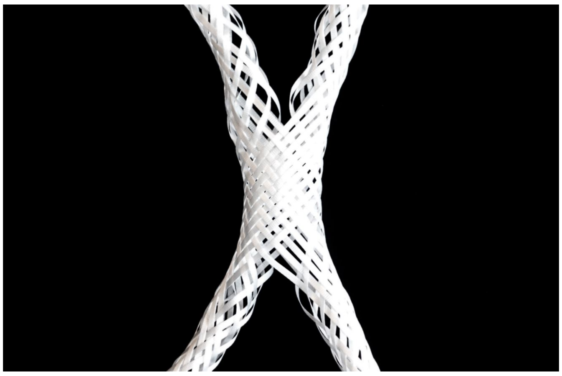

Figure 11: The braid is created from a machine configuration made from two connected circles where three tracks can be chosen. One track go around both circles, whereas the other two remain in their respective circular area. The program made such that firstly the carriers are assigned to follow the small circular tracks, then the one combined track, then again the separate tracks.

12 servos are mounted in a casing of minimized size. Each servo arm is replaced by either a winch wheel or a customized arm for pulling a string attached from the place of actuation to the servo. The entire servo casing fit inside the braided central body, see Fig. 12. The 12 strings go from attachment in servo arm, through small inlet holes in the casing, through the braided structure in a triaxial direction until the reach the filament attachment disk at the end of the limb where they are attached with an adjustable tensioner.

To control the 12 servos an Atmel Mega324u controller is via I2C communication controlling a 16-Channel 12-bit PWM/Servo Driver. The control program on the main micro controller is designed such that each servo can be given a simple *GoTo* command, and the current position is considered when adjusting the speed for all servos, such that the servo with the largest delta position moves fastest and the smallest delta position moves slowest, to arrive at *GoTo* simultaneously. This way gait controllers can be easily tested through imagining three or more positions for the servos, that in turn result in string lengths.

Designed vs Evolved gait controllers. A few attempts were made to manually design gait controllers on this basis, however with limited result. Another attempt was made to evolve a gait controllers using a generational evolutionary algorithm with tournament evaluation (see Fig. 13). Populations of controllers were each evaluated twice with the delta distance of body center movement. To evaluate the body movement we used camera vision on QR codes attached on to the body and to the surrounding arena. The evaluation failed in part because the quadruped

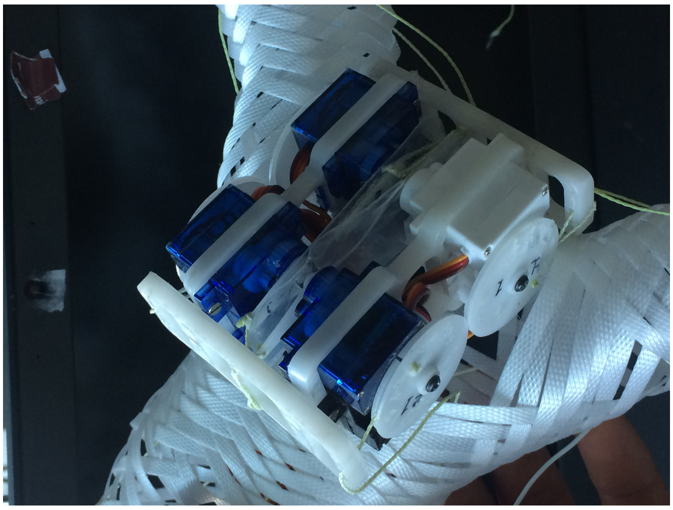

Figure 12: 12 servos with custom winch and servo arms compressed together in one casing. 12 strings attached individually to the servos connect the actuation to the end of each of the four limbs. One to pull the lower point, one to pull left and one string pulling the limb right.

fell over to its side such that the legs could no longer support the body. The evolution would however still evolve controllers for the new condition, but as the robot reached the rim of the arena, there would not be a strategy for turning, and the evolution halted.

Main point of failure for both the manual and the evolutionary strategy was the robot falling over to its side, resulting in legs being pulled together under the bottom part of the body. Had the robot had constant 3 legs on the ground at all times it may have had better stability and thus better gait. The quadruped moved at a speed of about 3 meters/hour. In evolution the quadruped moved to the wall of the arena where it collided and got stuck.

3.3 Twisted polymer fibers as artificial muscles

Actuated retractable filaments can improve the resilience of the braided structures. Therefore, we designed filaments inspired by the work of Haines et al. [5] using various polyamide fibers to create artificial muscles. The fibers shrink when heated and expand back when cooled. We used 82 cm of 0.5 mm polycaprolactam (PA6) and 0.12 mm NiChrom as heating wires. The fibers and the heating wires were attached to a controlled DC motor at the top, and a 270 g weight at the other end. A conductive rubber cord is connected to the end of each filament as a stretch sensor to measure the force applied to the filament. High resistance indicate a stretch force on the filament. The NiChrom is then heated accordingly to pull back and compensate the applied force and partially retract the filament to the former state (see Fig. 14).

3.4 NiTinol Nichrome composite distributed actuators

The composite actuator was created for the purpose of distributed actuation located at intersections of braided structures made from semi-rigid members.

The alloy NiTinol, also known as shape memory alloy was chosen because it can be activated thermally to change material properties of stiffness and spring back to an encoded shape, which in our case is a straight shape. For heating NiTinol a normal approach is making use of the internal

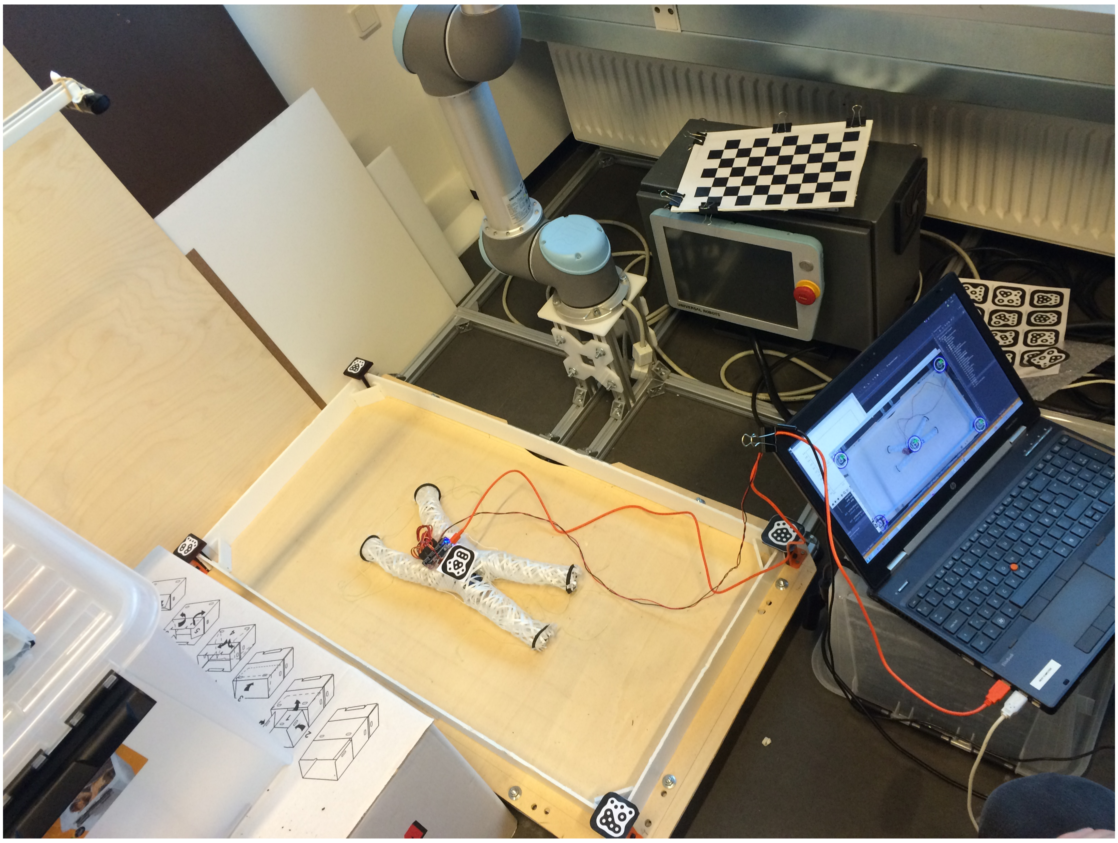

Figure 13: The braided quadruped in arena with video tracking via QR code. Tracking evaluate each locomotion controller with a delta distance. The USB cable transmit new controller settings to the robot, while the laptop runs the evolutionary algorithm based on the results of locomotion.

resistance of the material, however for this 1 mm thickness we found the internal resistance of was only $0.2\,\Omega$ resulting in a demand high currents when heating. Such levels of current are unsuitable for ordinary electronic applications. To get around this challenge of low internal resistance the wire is electrically insulated using heat-resistant polymide tape and a Nichrome wire of diameter 0.1 mm wrapped helically. 6.7 mm Nichrome thread is used for every one millimeter of NiTinol wire, see Fig. 15. The resistance for a 20 mm actuator using Nichrome diameter 0.1 mm is measured to about $30\,\Omega$ which correlates with our experimental data. More in depth analysis of SMA thermo-mechanics is documented by Mizar [6].

When applying the newly developed composite actuator to a single member of GFRP rod of diameter 1 mm the actuator would within 3 to 4 seconds of activation change the intersection angle between rods up to 60°, see Fig. 16. A larger braided structure similar to the GFRP 3 DOF manipulator is planned to have n composite NiTinol actuators distributed across its braid intersections allowing for a higher degrees of freedom manipulator.

Experiment measuring the strain of a composite NiTinol Nichrome actuator. The composite actuator reacts significantly faster than the equivalent length of bare NiTinol wire due to the activation of surface area in which the active force transmission takes place in similar structures. To test the strength of the actuator in relation to activation time and power

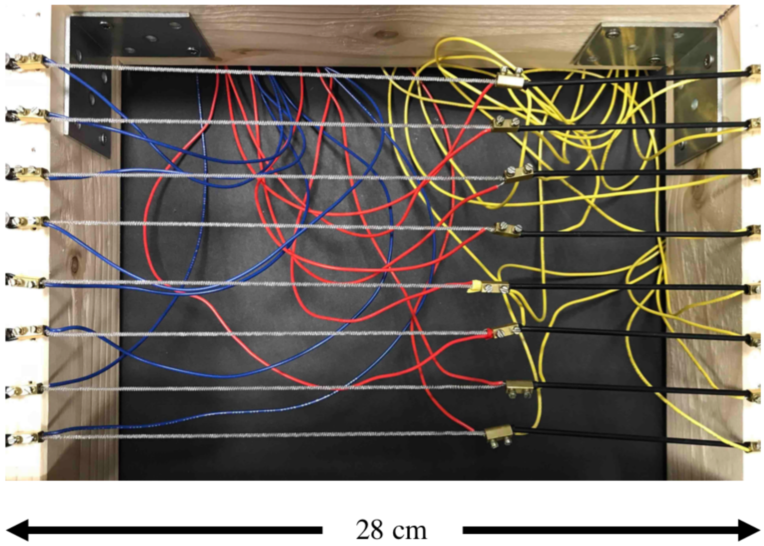

Figure 14: Eight polymer fibers coiled with heating wires in serial with stretch sensors.

consumption we measured static forces using a setup where the actuator applies forces to a scale.

The composite actuator is mounted in a non-conductive vice with anode and cathode attached at opposite ends of the helical Nichrome wire. The vice grips the actuator such that the bending moment is focused at the middle part. The actuator is initially deformed to 90° deformation at room temperature. While applying electrical power the Nichrome wire heats up the outer layer of the NiTinol wire causing a change in material properties causing the wire to attempt to spring back to its original straight shape. These spring forces were measured to be 1.2 N/cm. The power supply set to 12 V measured 0.4 A for 6 seconds, at which point a force of about 4 N or 2 N/cm was read on the scale, see Fig. 17.

3.5 Conclusions

There are several ways of actuating braided structures from soft filament and rigid rods. We have tested a few of the most commonly used and a few less traditional ones. The more conventional ones are servo and stepper motors, where steppers suffer from the lack of closed loop feedback, whereas the servo motors have in-build closed loop but suffer from fragile and inflexible mechanical adaptation. These two have a form-factor that contradicts the lightweight filaments they actuate.

The less conventional ones, artificial polymer and composite shape memory wire, are immediately more appealing to incorporate into braided filament structures due to their light weight, their capacity to distribute over the filaments, and their low emission of sound. The two types are also easy to handle electronically, but so far only the twisted polymer have been tested with closed-loop control. In the near future, prototypes with distributed composite SMA/Nichrome actuators will be tested to determine if this approach allows higher degrees of freedom in movement of a braided structure.

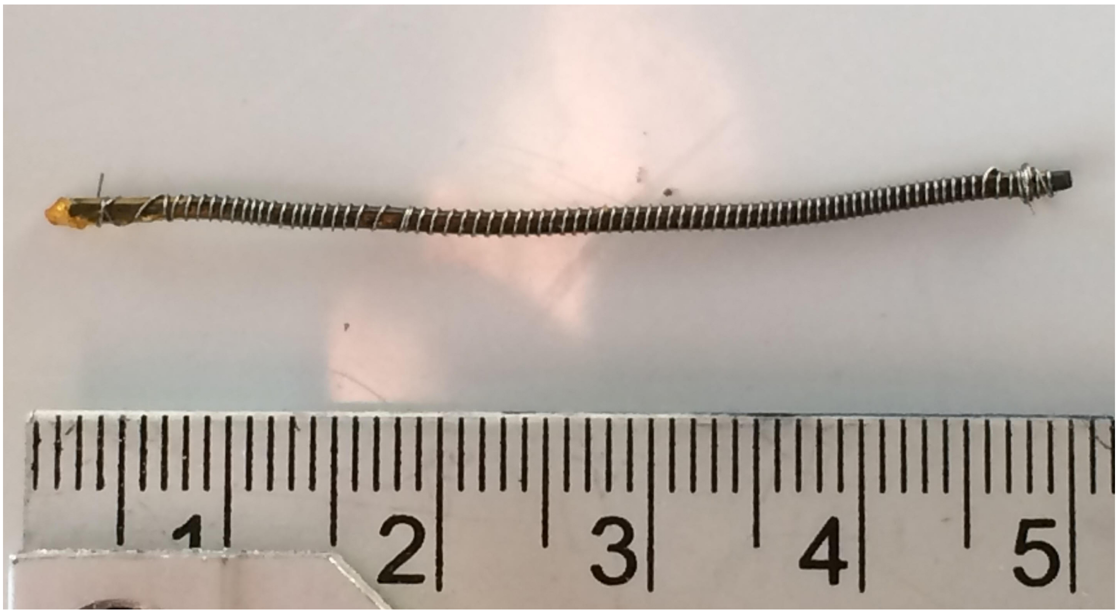

Figure 15: Detailed view of the composite actuator made from diameter 1 mm NiTinol wrapped in heat resistant polymide tape and Nichrome wire diameter 0.1 mm helically at 6.7 mm/mm.

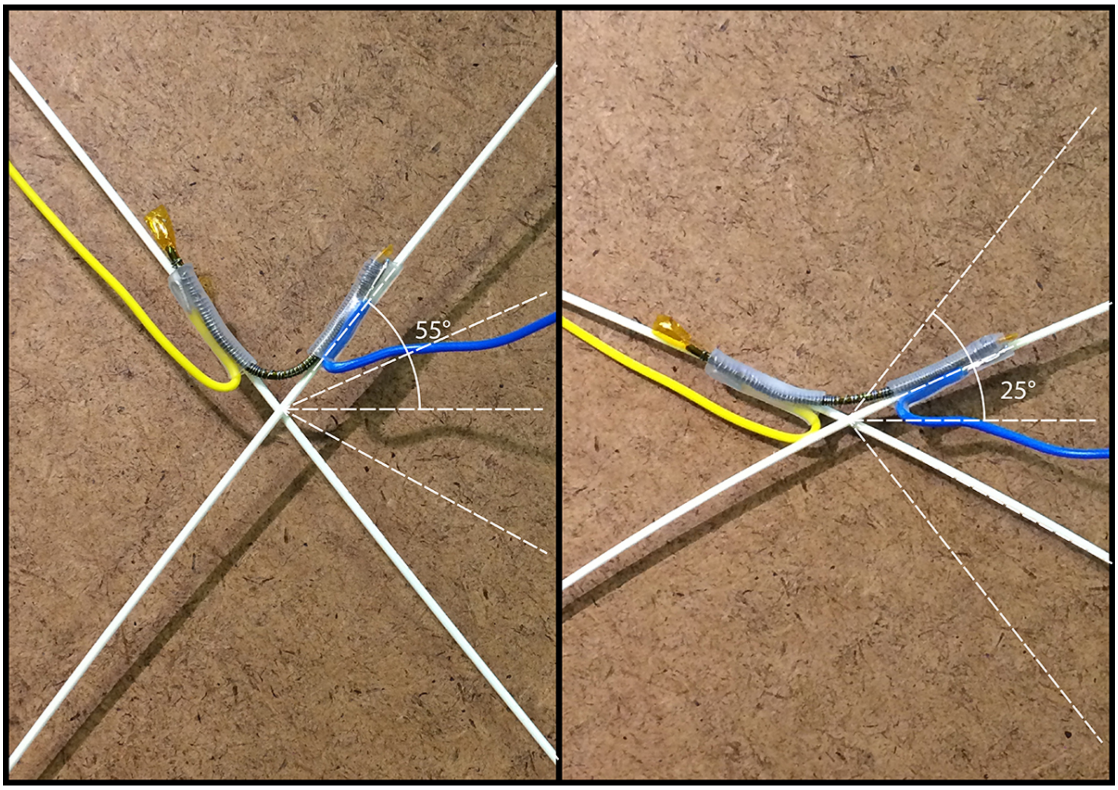

Figure 16: Detailed view of the mounted NiTinol and NiChrome composite actuator. It is connected to the GRFP rods and power leads through a single overlapping piece of silicone tubing. Left; The actuator straightens out to a degree where it counteracts the bending forces in the braid. The actuation results in an angular change of 60 degrees between the rods.

Figure 17: Measuring setup for the force of a NiTinol - NiChrome composite actuator of 60 mm spread bearings also acting as conductors to transfer power to the NiChrome wire. We observe a force of 4N, and an electrical power consumption of 0.7 A at 12 V during a time of 4 seconds from cool to heated and full force. from no force at 90 degrees deformation to full force 4 N. Summarized energy spend is about 28 joules, however we did not make measurement on the work the actuator can perform from this energy consumption.

Figure 18: Large braided structure at AMU, built during workshop in May 2017.

4 Actuation: Robots - Plants

Braided structures were found to be crucial element of *flora robotica* biohybrids. Their shape, topology, way of producing are still under continuous development, but even transient versions of braided structures were worth to be tested for their suitability for supporting plants growth. In D2.2 we showed that beans effectively used tower-shaped braids as scaffold in room conditions.

4.1 All Braid Structure

Now we have produced greater braided structures which were tested as a support for different species of climbing plants. In the case of climbing plants braided structures can provide fundamental resource, that is a scaffold, that is indispensable for developing climbers morphologies. Moreover, utilization of scaffold together with usage of growth-guiding robots will make possible, according to our assumptions, to obtain architectural significant artifacts. Braided structures might be find as type of actuation that is being implemented in *flora robotica*.

4.1.1. Big Braided Structure for support

The big braided structure was made during *flora robotica* workshop in May 2017 in hall of Faculty of Biology AMU. The structure is dangled from side hall's walls and mostly hang below

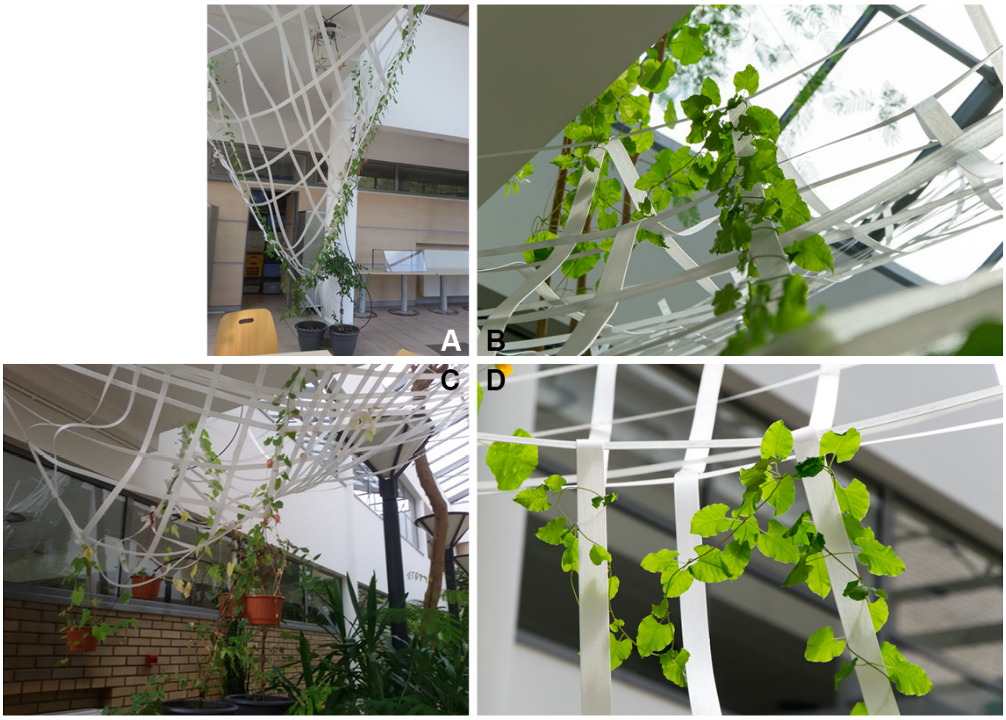

Figure 19: Climbing plants species in large braid structure. A) Fallopia and Lonicera; B) Fallopia and Nasturium; C) Common beans; D) Fallopia.

and nearby a bridge that is joining the two halls walls (see Fig. 18). Different climbing plants species were grown there: honeysuckle, *Fallopia aubertii*, nasturium, common bean. All of them have found braided structure and environmental conditions as suitable for their growth from spring to autumn. However, only twining plants species were grown. An ivy or a creeper, which glue to the support, were not grown there, due to concerns about their influence on a walls surface if overgrown. Fallopia was characterized by the biggest growth rate (see Fig. 19A, B). The common bean again proved its suitability for utilization of braid as support (see Fig. 19C). Some of the beans were grown in hanging pots below structure. The honeysuckle efficiently grew on the braided structure, however in the first year we did not observed any flowers (see Fig. 19D). Flowering was not observed for fallopia, too. It is mean that applied conditions were not appropriate for establishing plants full life cycle or, more likely, more seasons are required to induce flowering.

For establishing a semi-autonomous watering system, the Blumat automatic drip watering system[1] was utilized (see Fig. 20). The Blumat system depends on ceramic cones and watering pipes with regulated valves. Ceramic cones are responsible for adjustment of watering rate to soil moisture. No computer control and no electronic measurement of soil moisture is needed. Still, Blumat makes it possible to vary the watering for particular plants in the one system. The system autonomously responds to changes in the rate of drying of the soil. Using the Blumat system makes it possible to save electric energy and to avoid struggling with the implementation of any central control system. We use gravity for establishing proper water pressure, however, also electric water pumps could be used.

[1] https://blumat.com/en

Figure 20: Blumat automatic drop watering system.

Figure 21: Plants growing in large braid structure. A) Fallopia and Lonicera; B) Common beans, a poplar and dracenas; C) Lonicera and braided tower robot is visible; D) An effect of fast growth of Fallopia on the braid structure.

Figure 22: Fallopia and common beans growing on a small braided structure in our greenhouse.

4.1.2. Small Braided Structure for support

A braided structure stretched into a 2D rectangular surface was used as vertical scaffold for plants in a greenhouse. We tried to cover the whole braid surface with plants. A single fallopia quickly overgrew the braid but did not cover the braid over the whole width (see Fig. 22). Even pruning the shoots of fallopia did not induce broadening of the surface covered by fallopia. One common bean plant covers a bigger surface area than the fallopia due to its bigger leaves and despite having only one shoot in comparison to five shoots pf fallopia. Growing plants on braided structures may hence require different plant species for different goals:

1. plants may function as construction elements that mechanically strengthen, stiffen, or stretch a braid

2. plants may be used as ornamental elements that cover scaffolds, which provide an attractive shape, subsequently “realized” by plants

3. plants may provide other advantages, such as production of oxygen, attracting other organisms (humans, insects, fungus), filter the air (however, mainly root systems are relevant then)

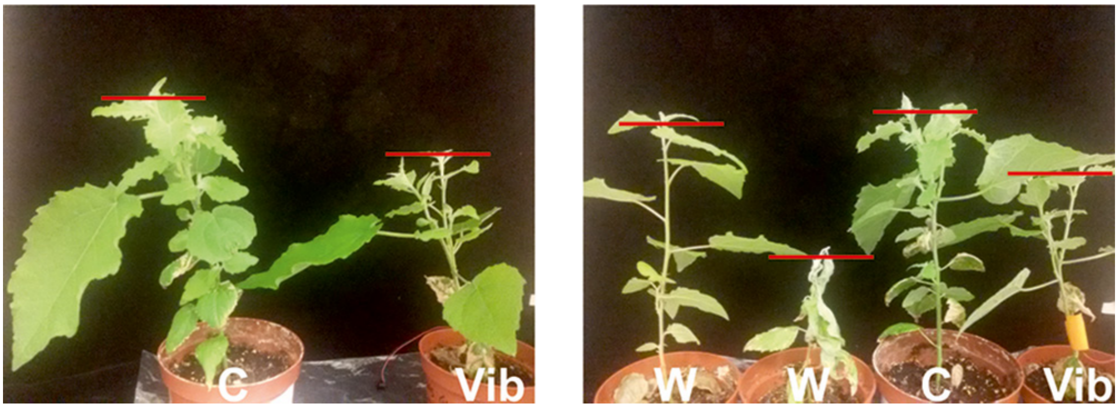

Figure 23: Poplars used at vibration experiment. *C* are control plants, *Vib* are vibrated plants, *W* are plants subject to wind. Vibrated plants were shorter, those subject to "wind" are a bit shorter, but some broke.

The different goals and functions of *flora robotica* systems influence the choice of species, as well as, environmental conditions and suitability to grow together with robots and braided structures. To provide structural material, trees could be used, example species can be found in D3.2, Sec. 4.2.3.

4.2 Vibration as actuation

In nature, mechanical stimulation, such as wind, leads to change in the architecture (shorter, thicker stem) and strengthening of the stem or other organs. In D2.2 we presented an introduction into middle scale cultures of poplars (12 plants) that were actuated by vibration motors in a greenhouse. Unfortunately, the culture was terminated by massive invasion of spider mites in June 2017, what prevent us from getting any reliable results from this experiment. We have continued the work with mechanical stimulation, which is feasible to implement and can be applied to plants by robots. We have investigated the influence of vibrations on different plant species.

4.2.1. Vibration motors experimentation

The new experiment with poplars and vibration motors was conducted in room conditions and on a smaller scale. Only 7 young plants in total, due to infected greenhouse and loss of previous generation of plants. Utilized poplars are propagated in *in vitro* conditions and their propagation is workforce intensive and time consuming. Fig. 23 shows results of two weeks of applying "artificial wind" or vibrations to young poplars. "Artificial wind" was generated constantly by a fan (Fander Roxo 8025H 80mm FRX3-8025H 2500 rpm) from 20 cm distance. Vibrations were generated by vibration motors (Precision microdrivers nr 304-116) every hour by 5 minutes. The MU board by CYB and Raspberry Pi Python script were used to control vibration motors, see Fig. 23. A control plant (C), that was not subjected to any stimulation grew taller than the plants subject to vibrations (VIB) or "wind" (W). The measurements of the chlorophyll level (ForceA) and transpiration level (Decagon SC1 porometer) were done during experiments. We did not observed any significant difference between actuated and non-actuated plants (data not shown). One of two example poplars subjected to "wind" stimulation is an example of a potentially deadly effect of mechanical stimulation (see Fig. 20). Due to insufficiency of room

Figure 24: A) Dracena subjected to vibrations. No effect was found during time of observation, that is, growth rates of branches were the same; B) Deformation of a poplar's stem after a few month growth with an attached vibration motor; C) Sunflowers require mechanical stimulation to develop self sustainable body. On the left sunflowers subjected to "wind", on the right sunflowers that were growing in room conditions without any applied air-flow; they cannot sustain their own weight.

conditions for establishing proper growth and development of poplars in long time, we were unable to monitor mechanical properties of poplars subjected to vibrations. We concluded that the same stimulation as mentioned above has no significant effect two months later at which time vibrated plants were growing in the same rate as control (data not shown). Long presence of vibration motor in proximity to stem (April until August, 2017) led to overgrown of device by plants tissue (see Fig. 24B). The incorporation of artificial elements by plants has to be considered in long term run of plants bio-hybrids.

4.2.2. Windflow as vibration actuation

Sunflowers, representatives of monocots, characterized by long, straight, and stiff stems were also subject to "wind" in room conditions, for example, deprived of any additional and prominent air flow. The plants, which were not subject to "wind", developed nonfunctional stems, broke down, and flowered prematurely (see Fig. 24C left). Sunflowers that were subject to "wind" were successfully growing and their stems supported straight vertical growth (Fig. 24C right). Hence, some plants require mechanical stimulation as an indispensable developmental factor.

Experiments with application of vibrations were done also with dracena. We studied four branches of similar morphology and investigated the influence of vibration motors on chosen organs of a plant. After one month of stimulation of two of the four branches, the dracena plant was growing more into the undisturbed direction (see Fig. 24A). Growth rates of each branch were the same, hence the vibrations had no influence on growth rates of the dracena branches. An alternative explanation can be that vibrations that spread across different dracena organs are strong enough to influence growth of each branch in the same way. Differentiation between these two reasons requires more experiments with additional control, which will be started in spring 2018, when the growth rate of dracena will be big enough again.

As a conclusion we have to stress that there is a need for adjustment of the applied mechanical stimulation methods to each plant of choice. Additionally, effects of mechanical stimulation differ between species and developmental stages. Also note that a common bean was shown to not being influenced by vibration motors, hence for this species we have to find another second stimulation (see D2.3). For some plants, in indoor conditions, mechanical stimulation will be necessary as well as additional light to provide an environment suitable for the plant's development and growth.

5 Sensing: Plants - Robots

In order to create the basis for interactions between plants and robots, data about the state of plants are needed. The different types of sensors applicable to plant parameter measurements as well as the development of the hardware and software interfaces were presented before in deliverables D1.1, D1.2 and D2.1. Now we give an update and report the current status of the *CYBRES phytosensor System* that is developed and used in *flora robotica*.

5.1 Phytosensing System

The current version of so-called *CYBRES Phytosensor System* device is shown in Fig. 25. The device receives power from and exchanges data with a PC using the USB interface compatible with the USB 2.0 standard.

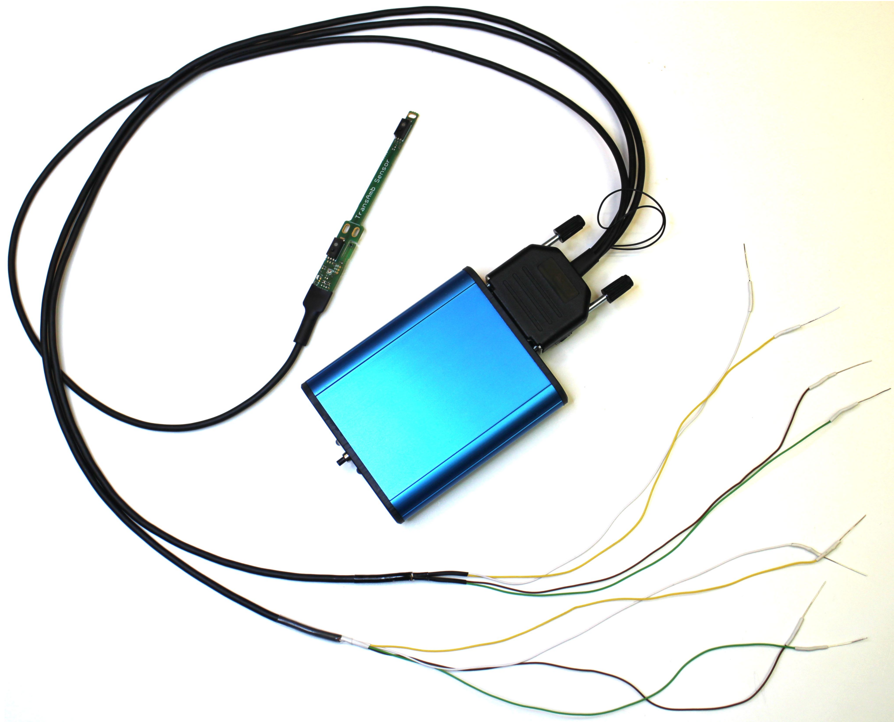

Figure 25: CYBRES Phytosensor System based on the MU3.3 device with measurement electrodes and transAmb stick sensor.

For this device we have written a **User Manual**,[2] which includes a detailed general description, measurement instructions, description of the operation modes, the functionality of *CYBRES EIS Client* program for Windows operating systems, options of graphical output for plotting and saving sensor data and more. The work on both, firmware and software, is still on-going as we are constantly improving, debugging, and adding new features, while periodically sending updates to users. The client program was tested and works with MS Windows 7, 8, and 10.

[2]CYBRES MU33 Phytosensor System User Manual
http://www.cybertronica.de.com/download/MU-EIS_Manual_en.pdf

5.1.1. Phytosensing Hardware

The Phytosensor itself consists of the following modules:

- MU 3.3 PCB with aluminum casing (see Fig. 26);
- needle type silver measurement electrodes (see Fig. 27);
- TransAmb sensor stick (see Fig. 28).

(a) Standard small aluminum case, size: 81 × 72 × 19 mm.

(b) Bigger aluminum case with enhanced thermostabilization, size: 120 × 78 × 43 mm.

Figure 26: A simple example of machine configuration and a simple output in simulation

The current version of the MU (Measurement Unit) is MU 3.3. The devices were produced and manually assembled in summer 2017 in limited quantity. Five devices were delivered to project partners (one Phytosensor for each partner) in October 2017 (see Fig. 29). The work on the hardware is still on-going. At the moment (Jan and Feb 2018), we perform different pre-compliance tests of the hardware in order to comply with EMC requirements for Information Technology Equipment (ITE), namely standards CISPR 24 (Information technology equipment - Immunity characteristics - Limits and methods of measurement) and CISPR 32 or 22 (Electromagnetic compatibility of multimedia equipment - Emission requirements).

We prepare the next production run of the MU 3.4 hardware, which will be produced in higher quantities. We are planning to order PCBA (Printed Circuit Board Assembly) production and component assembling at PCB Manufacturing Company.

Phytosensor posses following functionality:

- ▷ Plant Physiology Measurement;
  - Electrophysiology:
    - 2 Channels Tissue Impedance EIS (Electrochemical Impedance Spectroscopy);
    - 2 Channels Biopotentials;
  - Transpiration Rate (Differential Humidity);
- ▷ Environmental Measurements:
  - Temperature;
  - Humidity;
  - Ambient Light;

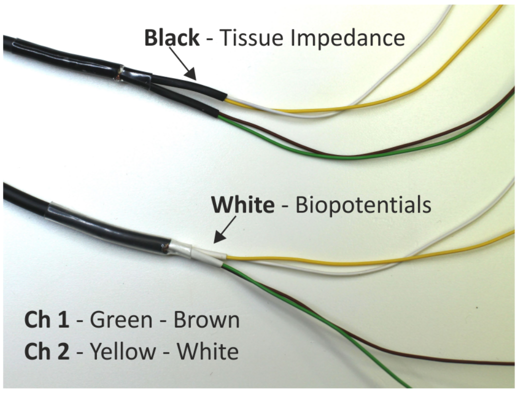

(a) The impedance and biopotentials measurements electrodes. The channels and types of electrodes can be recognized based on the color marking: shrink tube color; wire color.

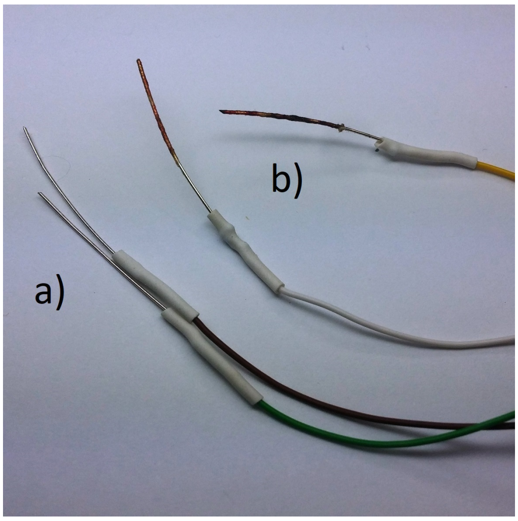

(b) The a) new silver-needles electrodes and b) silver-needles electrodes after the 3 month of continuous Cactae plant tissue impedance measurement affected by oxidation.

Figure 27: Needle type silver electrodes used for plant tissue impedance and biopotentials measurements.

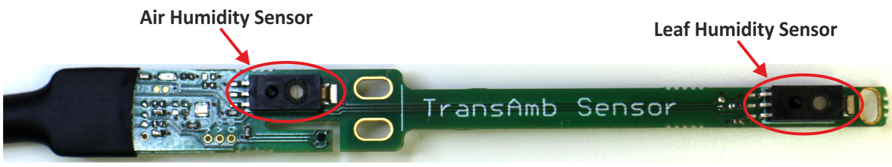

Figure 28: TransAmb sensor stick - the sensor PCB equipped with temperature, humidity, ambient light sensors and plant leaf transpiration rate measurement sensor.

Figure 29: 5 pieces of CYBRES Phytosensor System packages delivered to partners at the end of year 2017.

- RF Power (50 MHz - 3 GHz);
- Air Pressure;
- 3D Accelerometer, 3D Magnetometer;

▷ Additional Features:

- PCB Temperature Stabilization;
- 3 Channels of Actuation (Light, Water, etc.)[3];
- USB mini-B connector, Power and Data via USB Cable;
- ASCII-symbol-based command/data communication with external devices, USB-UART interface.

The transAmb sensor stick is a tiny PCB equipped with temperature, ambient light, and two humidity sensors, one for air humidity and a second for leaf humidity. The differential humidity measurements are used to determine the transpiration rates of plant leaves. The transAmb stick is a more technological version of the transpiration sensor prototype we had presented earlier in D2.1. In comparison to our previous prototype we use differential humidity measurements to get the information about transpiration rates. We have discarded the use of differential temperature measurements due to low signal-to-noise ratios and low reliability when measuring transpiration rates.

The needle type silver (0.25 mm diameter) electrodes are used for electrophysiology measurements. The electrodes are supposed to be injected into plant tissue in order to perform the measurements. The electrodes have color markings to allow to distinguish the types of measurements and between channels. Markings are:

▷ Tissue Impedance - **Black** shrink tube on cable;

▷ Biopotentials - **White** shrink tube on cable;

[3]In most cases additional power supply required by reason of USB 2.0 power limitation.

- ▷ Channel 1 - **Green (+) - Brown (-)**;
- ▷ Channel 2 - **Yellow (+) - White (-)**;

The pair of electrodes (channel 1 or channel 2) for tissue impedance measurements need to be mounted approximately betwen 15 and 25 mm away from each other. The polarity of electrodes for impedance measurements is not relevant because an AC voltage signal for excitation is used. Channels 1 and 2 can be injected far away from each other because the measurements are fully independent between the channels. The measurements for different channels can be performed in different branches or even in different plants. The impedance measurement is necessarily an invasive method: low AC voltage signals are put on tissue by electrodes, then the current between them is measured. The used voltage signal is relatively small (± 25 mV) in most cases. Nevertheless, in long-term measurements, such as two or three months or even more, this may cause visible injuries on the plant tissue. It is possible that the electrodes may get covered with organic tissue and a corrosion/oxidation film. This would change the electric contact property and also the result of measurements. So, for long-term measurement it is advised to check the electrode conditions periodically and to provide the required maintenance. In the case of the biopotentials measurement electrodes there are no such problems.

The electrodes in the pair (channel 1 or channel 2) for biopotentials measurements can be injected far away from each other in the plant as relative voltage potential measurement are performed. The measured biopotentials is equal to:

- ▷ Channel 1:

$$V_{ch1} = V_{green} - V_{brown} \tag{1}$$

- ▷ Channel 2:

$$V_{ch2} = V_{yellow} - V_{white} \tag{2}$$

Best information about the plants can be received using tissue impedance measurements. There are a number of existing modes for tissue impedance EIS measurement:

- ▷ Impedance Spectroscope;
- ▷ Single Scope;
- ▷ Continuous at fixed single frequency;
- ▷ Continuous at multi-frequencies;
- ▷ Frequency Response Profile (FRP);
- ▷ Continuous FRP;

The *Single Scope* is a basic mode and should be used first, when the Phytosensor is connected to the plant. The excitation signal range, amplitude, amplification gain, filters coefficient, and other parameters should be chosen carefully and properly to get an optimal response from the system. Example measurements are shown in Fig. 31, where (b) shows optimal and (a,c) wrong picking of the amplification coefficient.

The *Continuous Frequency Response Profile (FRP)* mode is the most advanced EIS tissue impedance measurements mode. It uses wide range of frequencies between 0.1 and 200 kHz and a 3D heat map of RMS Impedance or RMS Conductivity, Frequency Response Analyzer (FRA) Phase can be plotted. The example of (a) Dracaena and (b) Cactae plant responses to a short heat impact are shown in Fig. 32.

5.1.2. Developed parts of firmware and client software

Software includes the firmware run on the MU device as well as the client part run on the PC. The basic part of the firmware is the real-time operating system MU OS developed by CYBRES for programmable-systems-on-chip (PSOC). The MU OS includes different device drivers, the measurement module, data processing unit, and tasks scheduler. The development started in 2013 and is currently used on different CYBRES devices. A specific module in MU OS is in charge of all phytosensing purposes and low-level data processing.

The user interface is shown in Fig. 30. This software system includes a plotting engine, the USB interface part, the MU OS terminal, and different modules (in particular for phytosensing purposes). The client program has six sections: 'control' (system control), 'impedance' (setting for the EIS measurements), 'plot' (setting for the graphical output), 'system' (system setup), 'calibration' (calibration settings), and 'output' (the output window of the operating system and some interactive commands). The client part is fully compatible with MU OS and is also used in different CYBRES projects and devices.

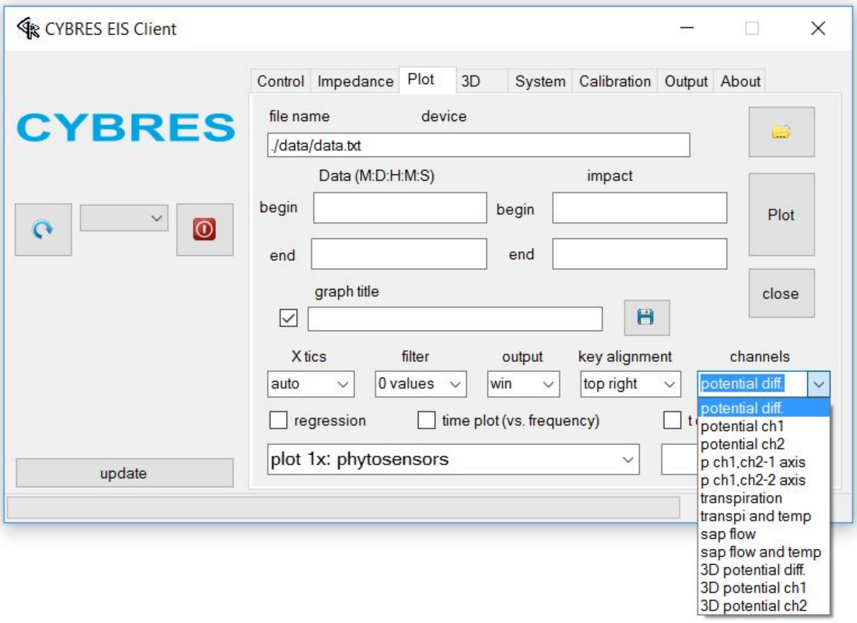

Figure 30: Client software with the option "phytosensors" and the list of available plots.

For the phyto sensing purposes a specific module was developed in the client program. It is integrated in the section 'plot' and maintains over ten different subsystems for data processing (also regression analysis for online data in the 'time mode'). Currently, the work is concentrated on developing algorithms and strategies for autonomous data processing, in particular electrophysiology.

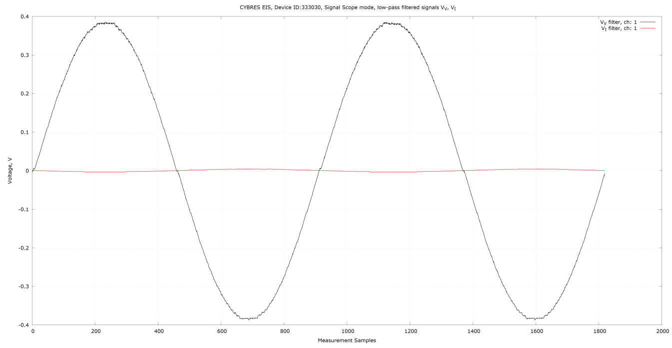

(a) Amplification 50, poorly chosen, response too low.

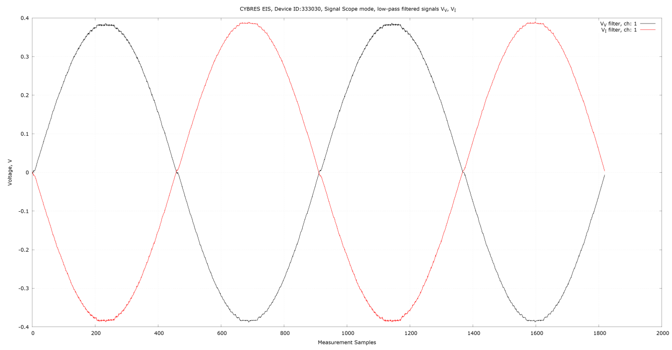

(b) Amplification 5000, correctly chosen, optimal response.

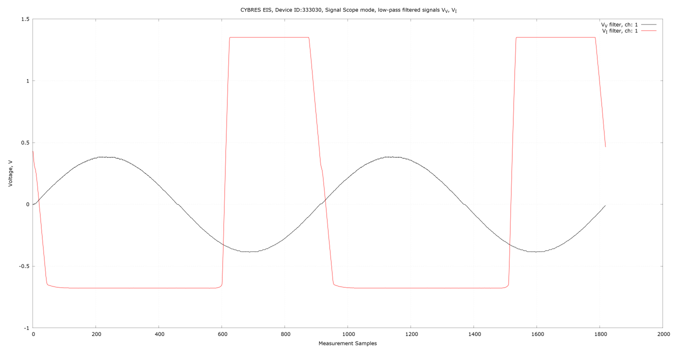

(c) Amplification 50000, poorly chosen, response signal saturated.

Figure 31: Tissue impedance single scope mode measurement. *Black* - excitation voltage signal. *Red* - amplified response current signal. Different amplification coefficient provide different dynamic range. Amplification coefficient have to be chosen manually properly.

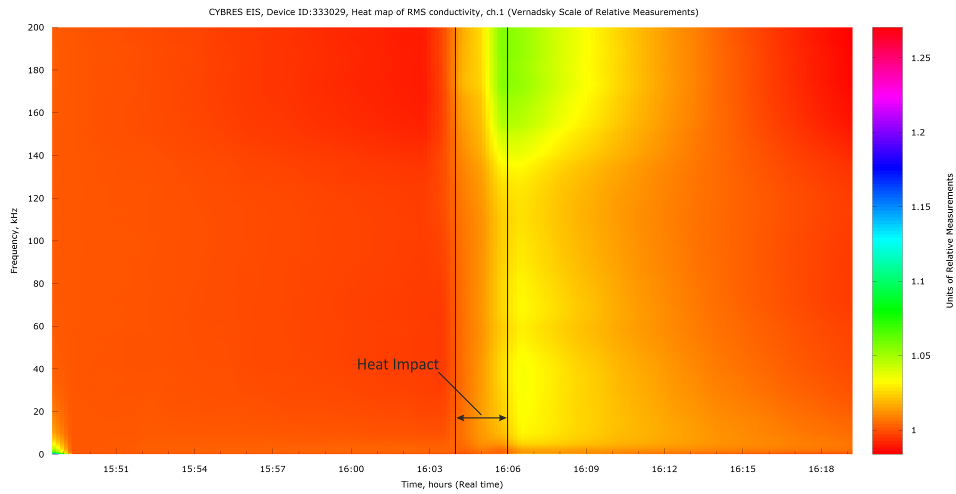

(a) The heat map of RMS conductivity of Dracaena plant tissues.

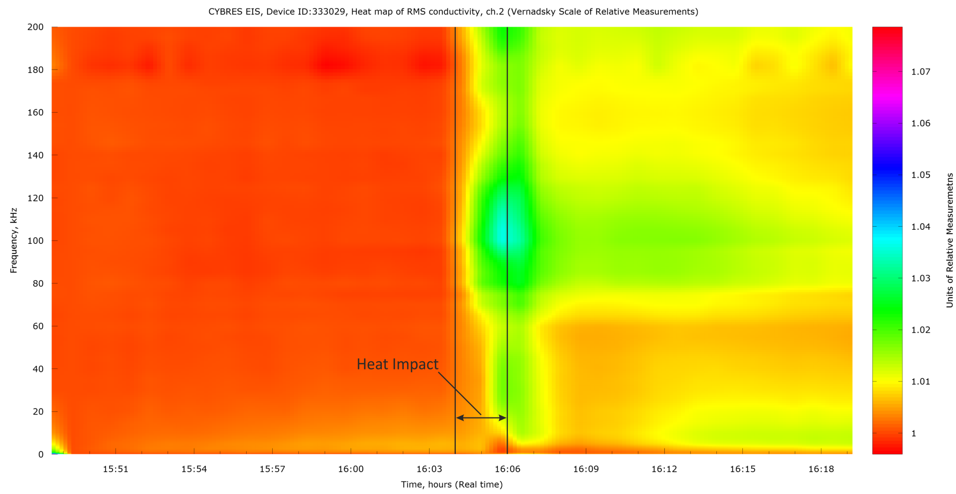

(b) The heat map of RMS conductivity of Cactae plant tissues.

Figure 32: The example of plants responses to heat impact applied with heat-gun from 1 m distance. The responses registered with multi-frequency (between 0.1 and 200 kHz) tissue conductivity measurement represented at relative scale.

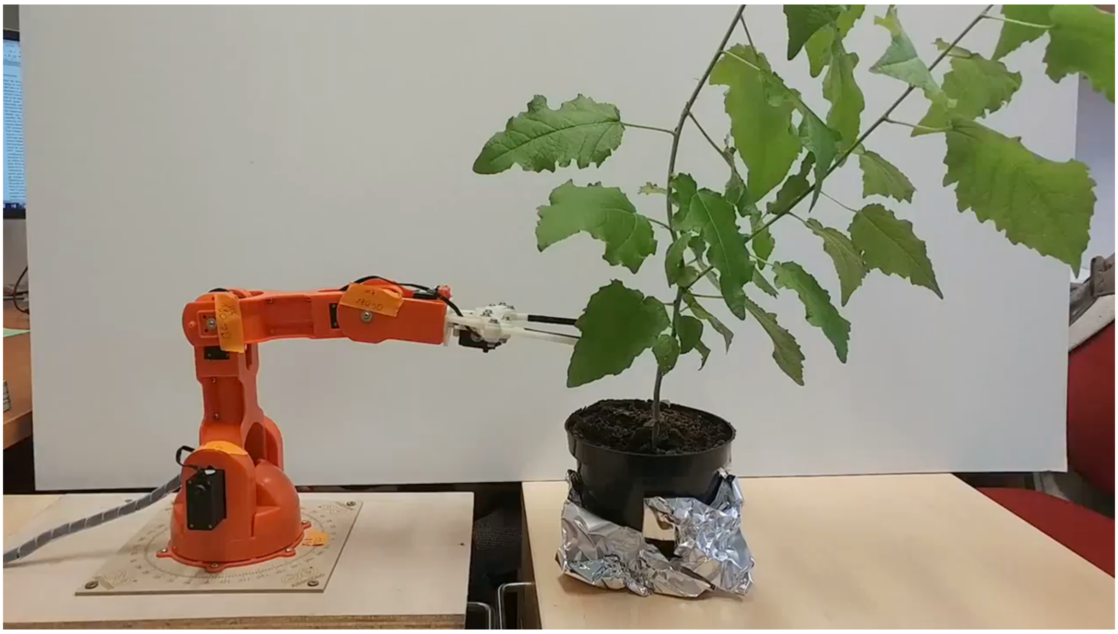

Figure 33: Braccio TinkerKit robotic arm acting on poplar.

5.2 Phytosensing in use

For *flora robotica* obtaining information about plants and environmental conditions is crucial. This information enables the system to adjust actions of our robotic nodes and other artificial elements in order to support the plants and to guide their growth. During plant guidance and shaping, the detection of an approaching plant is done by the robotic nodes. In addition, Phytosensors are our main devices to gain information and to establish an information flow from plants and their internal processes to robots. Having an insight into the internal processes of plants is required for establishing functional bio-hybrids. We need Phytosensors to guide the actions of our robotic nodes, while it is essential to not damage plant organs and to influence the plants appropriately. Here we present some preliminary results of sensing plant physiology with Phytosensors, which were delivered to AMU in the end of 2017.

We have focused mainly on Phytosensor responses to changes in short periods of time, such as destruction of a vicinal organ and touching or leaning of a plant. Generally, we want to investigate measurements on short and long time scales, but due to the limited number of available sensors we focused at first on rapid plant responses to different stimulations and changes in environmental conditions. Common beans are currently an important species in *flora robotica* and we used them for Phytosensor measurements here, too. Electrodes are easily inserted into bean organs. The use of electrodes for woody organs of trees or shrubs will require further development. The electrodes were not targeted at specific tissue but features of the organ scales were taken into consideration during insertions. It is important to ensure good positioning of the electrodes and possibly repeated tries to ensure that relevantly plant responses are measured for a given change of conditions or a stimulation. Electrodes were inserted into beans, if not mentioned differently, than the stem was the targeted organ with full or almost full penetration, with a distance between electrodes of about 3 cm. We present results of short time measurements of biopotentials.

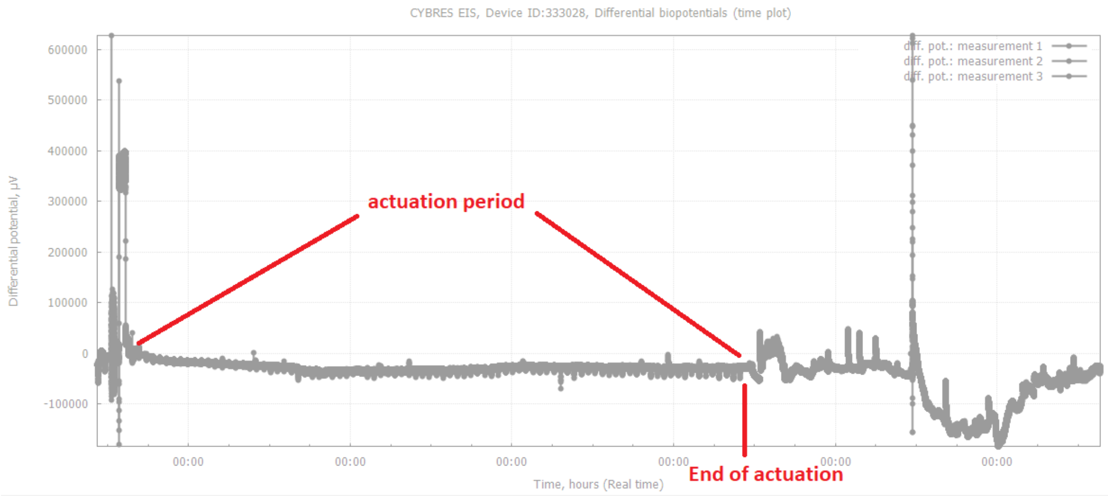

Figure 34: A mechanical arm (Tinker Kit Braccio) was used to lean a plant from vertical position to 45°. Actuation was programmed for every 60 minutes, but due to used simple delay command on Arduino, intervals between the arms action differs in range of ∼50-70 minutes. Both channels were cabled to one plants: the first to middle region of stem, below region of direct arms touch, the second into upper leaf. Differential potentials mode was used. Two the highest peaks correspond to beginning and end of actuation where some handling with plants was done.

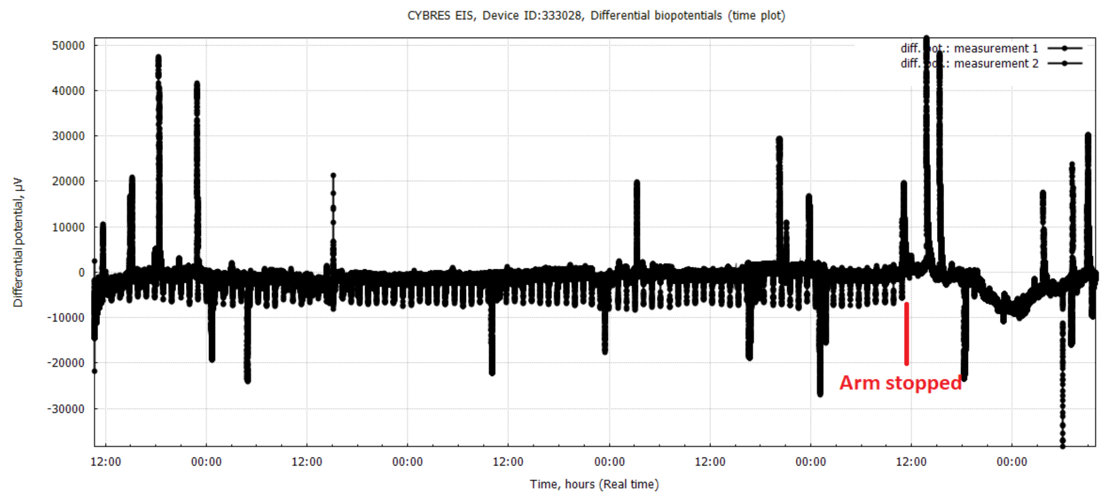

Figure 35: In this case poplar (0.5 m height, stem and one branch) was subject to Braccio arm stimulation. Points for electrodes insertion were restricted to softer plant organs, petioles in this case. The Braccio robot was stimulating once per hour and a plant was bent from vertical to 45°inclination. Regular decreases of differential potentials were measured in intervals of about one hour. Also irregular, bigger increases and decreases were observed, several of them correspond to switching the light on/off.

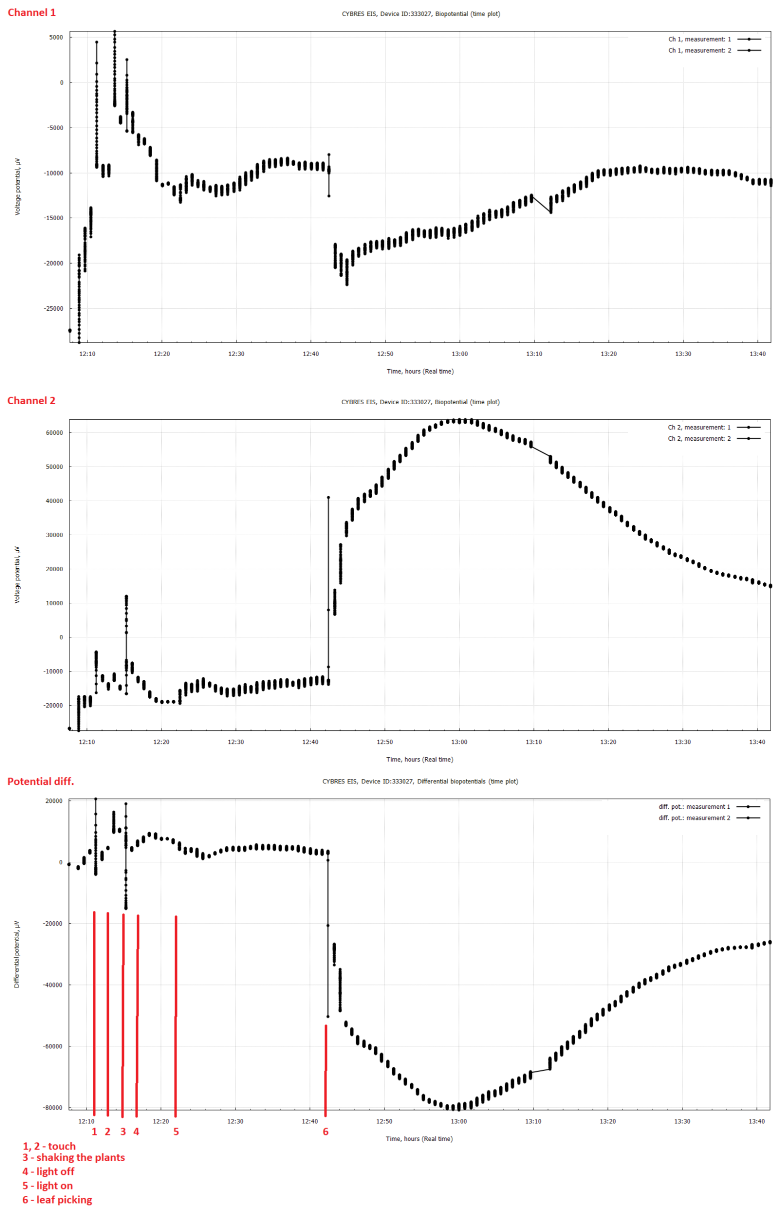

Figure 36: Few rapid responses to different stimulations were measured as differential biopotentials. Channel 2 was set on straight stem of a bean, Channel 1 was above, one electrode above and one electrode below a branching point on the main stem. Different localizations of channels electrodes strongly influence output. Most of stimulus generated greater decrease/increase in the case of Channel 1. Stimulations: touch, shaking, leaf cutting were done closer to Channel 1 than Channel 2. Leaf cutting generated the most prominent decrease of potential within the measurement for Channel 1 and the most prominent increase for Channel 2. Channel 1 was also closer to leaves, which are more light sensitive organs than stem. Hence, stronger response measured by Channel 1 than Channel 2 also seems reasonable.

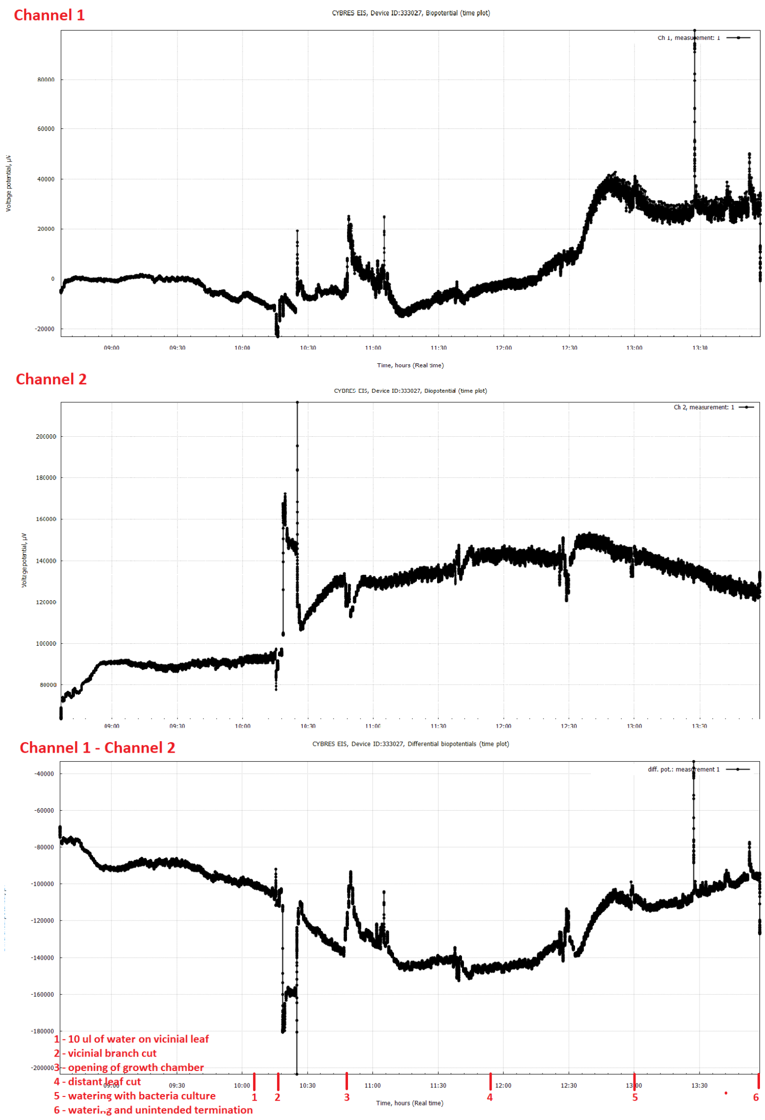

Figure 37: Few rapid responses to different stimulations were measured as differential biopotentials. Channel 1 provide information from electrodes inserted into main stem of a bean, Channel 2 from lateral branch above from Channel 1. First cut of leaf, which was close from Channel 1 electrodes resulted in big increase in Channel 2 and in slighter fluctuations of Channel 2. Second cut of leaf, the more distant leaf from both Channels than first cut leaf, resulted in smaller changes in measured biopotentials. Opening of growth chamber also produced more prominent response from Channel 2, which was closer to leaves than Channel 1.

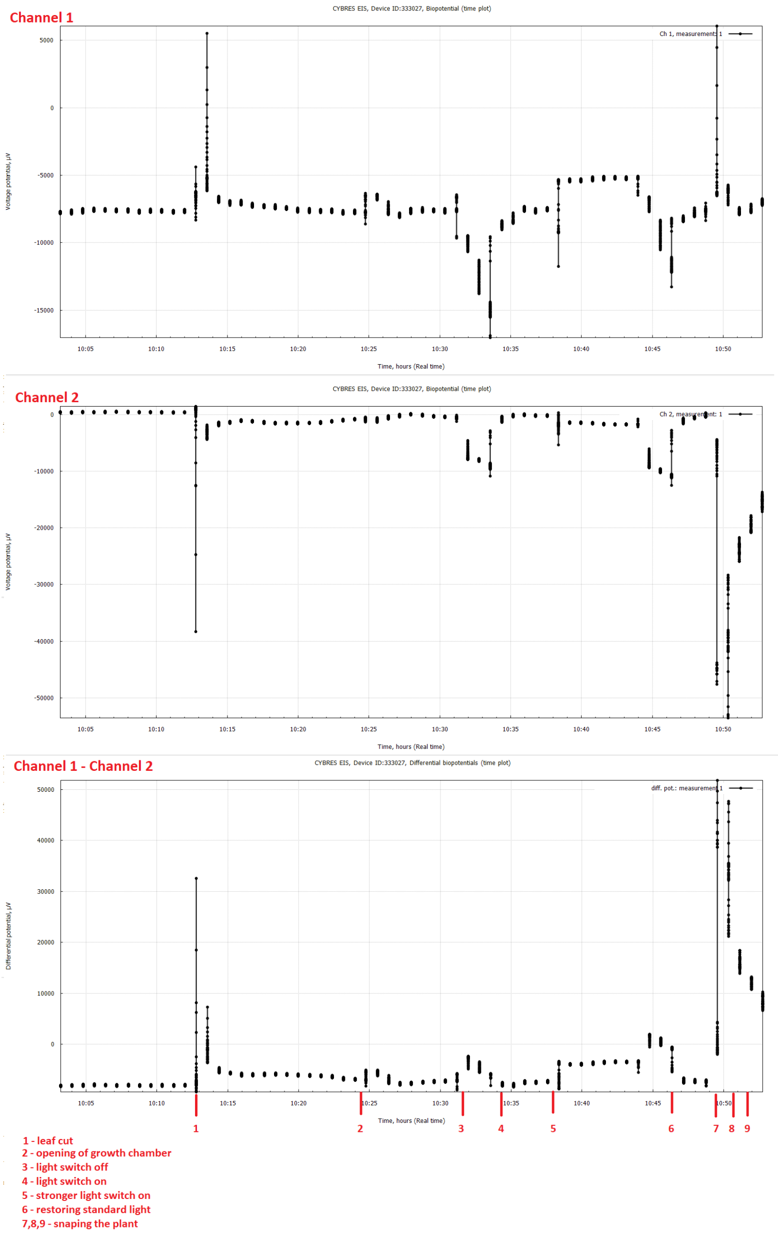

Figure 38: A Few rapid responses to different stimulations were measured as differential biopotentials. Both Channels were inserted into a stem. Channel 1 lower electrode was 2 cm higher than Channel 2 higher electrode. It is mean that they were close to each other in the same organ. Higher placed and the leaves closer channel, that is Channel 1, generated greater response to light changes. Surprisingly, a leaf cutting or clicking the plant's apex resulted in changes in biopotentials that were reversed, but of similar amplitude, between Channel 1 and Channel 2.

5.2.1. Short-term measurements

Please see Figs. 33, 34, 35, 36, 37, 38 and the respective descriptions in the captions. Different possibilities of using Phytosensor biopotential measurements were explored. Repetitive mechanical stimulation of a plant produced repetitive changes in the biopotentials. Termination of robotic actuation resulted also in parallel disappearance of biopotentials changes, so these changes did not continue due to internal processes of the plant. Channels that were closer to damaged organs, revealed greater response and biopotential change while a leaf was cut. Moreover, channels which were closer to leaves showed more sensitivity to changes in light conditions. However, we found that it may be hard to distinguish between different types of external events. Cutting leaves resulted in explicit increase/decrease of biopotentials, but from time to time explicit changes occurred due to unknown reasons. Cutting events provide a longer change, however, the observed strong increases and decreases may not allow for useful interpretations. Interestingly, the same event may correspond to the increase or decrease in the potentials. Plant shaking, snapping, and touching also clearly influences biopotentials, however, at lower levels than cutting. Moreover, also changes in light conditions clearly influence biopotentials, more strongly to channels closer to light harvesting organs, that is, leaves. No day scale response to watering/drying or the circadian clock were observed. Here, we limit our discussion of possible hypotheses because more experiments and a more sophisticated analysis are required.

5.2.2. Long-term measurements

We have not obtained a lot of results from long term measurements, which are probably of high relevance for *flora robotica*. One result is presented in Fig. 39. Unfortunately, we experienced that often Phytosensing measurements stopped after a few hours, when conducted in a growth chamber. We plan to study changes in a plant's architecture in long term measurements, going beyond the use of Phytosensing for monitoring environmental conditions and maybe the increase in biomass. The idea of EIS-branching detection rely on an hypothesis that EIS may be used for measurement of increase in biomass. EIS was shown to be useful for measuring root system in hydroponic cultures by Paavo Pelkonen lab [3, 4]. We want to focus first on the appearance of a new branch and changes of growth rates for different branches. To do so, more than one sensor for one plant is required. The more complex the plant's architecture is, the more Phytosensors we will need. Utilization of EIS for tracking plant architecture will provide an efficient supplement to the data gathered by the robotic nodes on detection of plant tips of growing plants. For plants of higher architectural complexity than a common bean (e.g., trees), the EIS may become even indispensable. Monitoring changes in biomass and occurrence of new organs are also important for shaping a perennial plant and to produce a bio-hybrid as an architectural artifact. More spatially relevant plants live long and show different types of architecture, *flora robotica* systems may hence require more complex sensing systems.

5.2.3. Future perspectives

As it was mentioned in D1.2, we need appropriate measurement and subsequent data analysis to obtain reliable insights into internal plants processes with Phytosensors. Such measurements will help to understand physiological processes and possible correlations between obtained measurement and external plant-affecting events will also turn out to be useful in *flora robotica* systems. Measurements conducted by Phytosensors will be of great importance to guarantee capable interactions between robots and plants. Applications of great numbers of Phytosenor may be indispensable solutions for keeping reliable and useful phytosensing in *flora robotica*. Constructing and coordination a network of Phytosensors will make it possible to exploit the

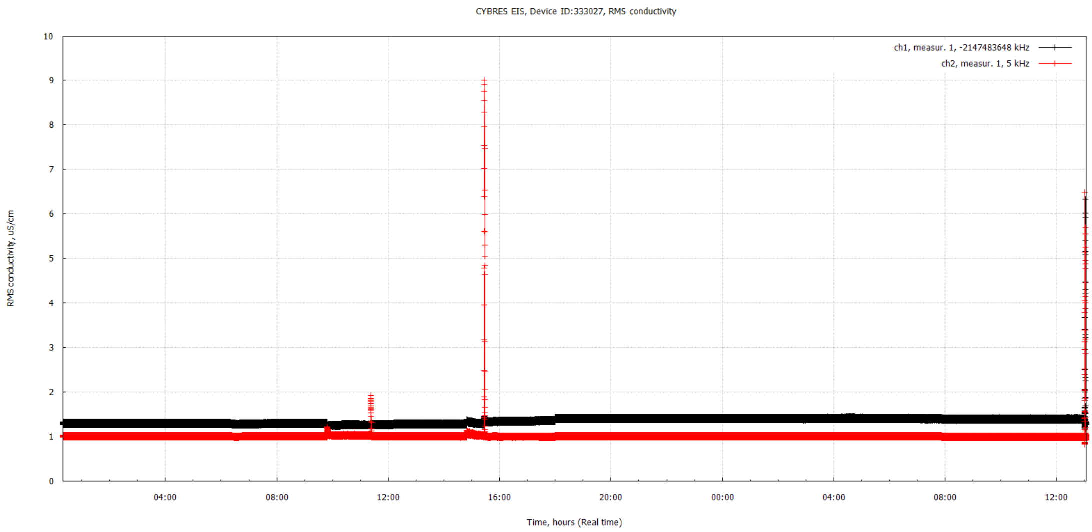

Figure 39: EIS measurement with two channels was conducted on a bean. Channel 1 was inserted in the stem, above Channel 2. Between electrodes of Channel 2 a branching point was present. Channel 1, "embracing" the branching point was characterized by greater increase in RMS conductivity, what might be a result of less complex architecture of "embraced" region. Unfortunately, this and other EIS experiments terminated prematurely, hence more work is required to prove the EIS-branching detection hypothesis.

potential of phytosensing. A spatial mapping of biopotentials changes within systems will enable us to differentiate between diverse types of events. Strong and irregular peaks, which do not correspond to any known relevant event, probably will be easier to be filtered. Damages have to be distinguished from non-destructive mechanical stimuli and they need to be localized to properly induce changes. With this functionality at hand, we will be able to detect damages to plants and to trigger appropriate actions to regrow plants in targeted areas.

6 Conclusion

This concludes the overview of distributed actuation and interaction mechanisms for robot-plant bio-hybrids. This last deliverable of WP1 has established the basis for interaction mechanisms and interaction through three separate system distinctions, namely 1) robot to structure, 2) plant to robot, and 3) robot to plant. We have accounted for our continuous development of the modular braiding machine for production of braided structures of different topologies and morphologies. The research into creating structures for the bio-hybrid in various materials seems to finally be successful. Secondly, efforts have been made to find efficient approaches for actuation of these braided structures. Here, we have reported on a series of approaches with different advantages and disadvantages. The successful bi-directional interaction and actuation proves the relevance of these findings for our further development of integrated demonstrators of the robot-plant hybrid as well as in social architectural settings.

References

[1] Kadir Bilisik and Nesrin Sahbaz. Structure-unit cell-based approach on three-dimensional representative braided preforms from four-step braiding: Experimental determination of effects of structure-process parameters on predetermined yarn path. *Textile Research Journal*, 82(3):220–241, 2012.

[2] Alexander Bogdanovich and Dmitri Mungalov. Recent advancements in manufacturing 3d braided preforms and composites. *Proc ACUN-4 Composite systems-macro composites, micro composites, nanocomposites. Sydney, Australia: University of New South Wales*, 2002.

[3] Yang Cao, Tapani Repo, Raimo Silvennoinen, Tarja Lehto, and Paavo Pelkonen. An appraisal of the electrical resistance method for assessing root surface area. *Journal of Experimental Botany*, 61(9):24912497, 2010.

[4] Yang Cao, Tapani Repo, Raimo Silvennoinen, Tarja Lehto, and Paavo Pelkonen. Analysis of the willow root system by electrical impedance spectroscopy. *Journal of Experimental Botany*, 62(1):351358, 2011.

[5] Carter S Haines, Márcio D Lima, Na Li, Geoffrey M Spinks, Javad Foroughi, John DW Madden, Shi Hyeong Kim, Shaoli Fang, Mônica Jung de Andrade, Fatma Göktepe, et al. Artificial muscles from fishing line and sewing thread. *science*, 343(6173):868–872, 2014.

[6] Shivananda Pai Mizar. *Thermomechanical characterization of NiTiNOL and NiTiNOL based structures using ACES methodology.* PhD thesis, Worcester Polytechnic Institute, 2005.

[7] Dmitri Mungalov and Alex Bogdanovich. Automated 3-d braiding machine and method, August 27 2002. US Patent 6,439,096.

[8] Kenneth O. Stanley and Risto Miikkulainen. Evolving neural networks through augmenting topologies. *Evolutionary Computation*, 10(2):99–127, 2002. URL http://nn.cs.utexas.edu/?stanley:ec02.